


## REVIEW

# Boosting Zn metal anode stability: from fundamental science to design principles

Zhen Hou | Biao Zhang 

Department of Applied Physics & Research Institute for Smart Energy, The Hong Kong Polytechnic University, Hung Hom, Hong Kong, China

**Correspondence**

Biao Zhang, Department of Applied Physics & Research Institute for Smart Energy, The Hong Kong Polytechnic University, Hung Hom, Hong Kong, China.

Email: [biao.ap.zhang@polyu.edu.hk](mailto:biao.ap.zhang@polyu.edu.hk)

**Funding information**

General Research Fund (GRF) scheme of the Hong Kong Research Grants Council, Grant/Award Number: 15307221

**Abstract**

The development of Zn metal anodes suffers from several critical issues, including dendrite growth, hydrogen evolution reaction, and corrosion. Extensive efforts have been applied through ameliorating electrode structures, electrode/separator interfaces, and electrolyte formulations. We deviate from the specific approaches and discuss the roots of the existing problems to exploit the fundamental science behind the proposed approaches. We divide the Zn deposition process into four steps, that is, mass transfer in the bulk electrolyte, desolvation on the electrode surface, charge transfer for the  $\text{Zn}^{2+}$  reduction, and Zn cluster formation through the electro-crystallization. It can be seen that all the reported strategies for improving Zn anode stability deal with at least one of these steps, thereby enhancing the understanding of dendrite formation and benefiting the rational design to circumvent the issue. We also scrutinize the previous attempts to suppress the side reactions through water activity reduction and electrode passivation to raise battery reliability. Finally, we propose possible solutions to the remaining but urgent challenges toward low-cost, high-safety, and long-lifespan Zn metal batteries.

**KEYWORDS**

dendrite growth, hydrogen evolution reactions, Zn metal anodes,  $\text{Zn}^{2+}$  deposition steps

## 1 | INTRODUCTION

The search for green and clean energy resources, such as wind, solar, and tidal, is attracting extensive attention worldwide.<sup>1</sup> Nonetheless, their efficient utilization is largely restricted by the inherent intermittence and dispersibility of renewable energy.<sup>2</sup> Electrical energy storage (EES) is a promising approach to capture the energy harnessed from these “uncontrollable” sources. Of existing EES technologies, rechargeable Li-ion batteries (LIBs) that possess prominent cycle life and high energy density have undoubtedly become a protagonist, especially in the

energy market of portable electronics and electric vehicles.<sup>3,4</sup> However, their application as a large-scale EES system is greatly plagued by several issues, including the limited lithium reserves, the high cost of raw materials, and safety issues related to the flammable organic solvents.<sup>5,6</sup> This dilemma has stimulated the researchers to seek alternative advanced battery systems featuring environmental friendliness, economic benefits, safety, and excellent cyclic stability/rate capability.

Aqueous rechargeable batteries (ARBs) have been regarded as one of the most promising candidates since the employment of water as an electrolyte solvent meets

This is an open access article under the terms of the [Creative Commons Attribution](https://creativecommons.org/licenses/by/4.0/) License, which permits use, distribution and reproduction in any medium, provided the original work is properly cited.

© 2022 The Authors. *EcoMat* published by The Hong Kong Polytechnic University and John Wiley & Sons Australia, Ltd.

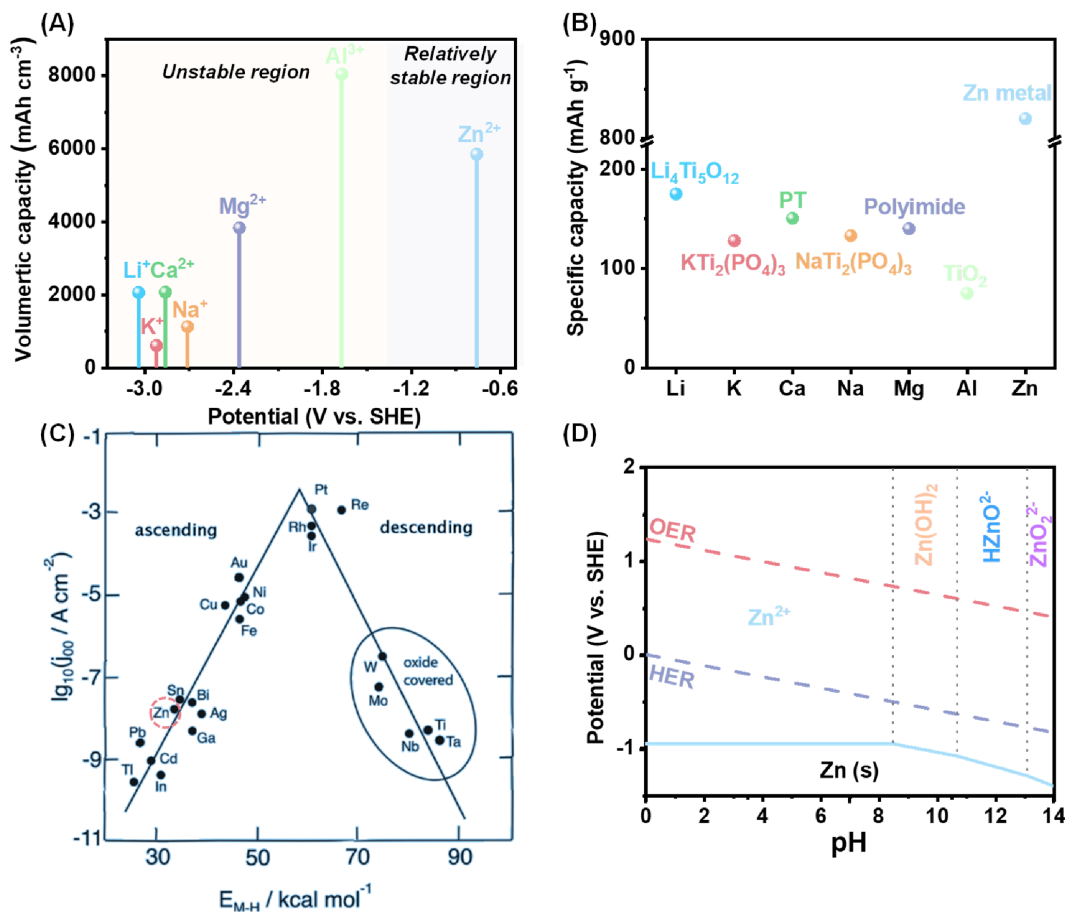


**FIGURE 1** Advantages of ZMBs. (A) The potential and volumetric capacity of various metal anodes. (B) The specific capacity of Zn metal anode and the typically available anodes in other ARBs. (C) Trassati's volcano plot for HER in acid solutions.  $j_{00}$  and  $E_{M-H}$  represent the exchange current density and energy of hydride formation, respectively. Zn element is located in the left bottom corner and has a low reaction rate, leading to a high kinetic overpotential over HER. Reproduced with permission.<sup>11</sup> Copyright 2014, Beilstein-Institut Zur Forderung der Chemischen Wissenschaften. (D) Pourbaix diagram of Zn in aqueous solution. Zn element is amphoteric metal where four different forms exist in an aqueous solution depending on pH. The concentration of Zn<sup>2+</sup> is 10<sup>-6</sup> mol/L in the calculation

the above demand.<sup>7–10</sup> Specifically, the cost can be highly reduced by utilizing cost-effective water solvent/water-soluble solutes and manufacturing ARBs under an ambient atmosphere. Water solvent is intrinsically non-flammable and nontoxic. Additionally, superior power outputs could be achieved thanks to the fast ion transport in aqueous media. Among various ARBs, zinc metal batteries (ZMBs) have received dramatically increasing interest, owing to the following merits: (i) Zn metal that is relatively stable in a humid environment without severe corrosion can be directly employed as the anode (Figure 1A), while other metals showing higher reactivity, such as sodium, potassium, calcium, magnesium, and aluminum, cannot stably exist in aqueous electrolytes.<sup>12,13</sup> Zn metal anode possesses a high volumetric capacity of 5851 mAh cm<sup>-3</sup> and a specific capacity of 820 mAh g<sup>-1</sup> (Figure 1B), which is considerably higher than the available anodes in other ARBs.<sup>14</sup> (ii) Zn foil as

an anode is commercially available. This can bypass the complicated electrode fabrication procedures, commonly consisting of mixing, casting and spreading of slurry and solvent evaporation, which helps reduce processing cost and boost processing efficiency.<sup>15</sup> (iii) The appropriate redox potential of -0.76 V versus the standard hydrogen electrode (SHE) and high kinetic overpotential for hydrogen evolution reaction (HER) concurrently guarantee a feasible Zn deposition/stripping process in aqueous electrolytes (Figure 1C).<sup>16,17</sup>

Current ZMBs could be divided into two groups based on the pH of their electrolytes (Figure 1D).<sup>14,18</sup> One is alkaline ZMBs where pH is >7.0, for example, Zn-air and Zn-Ni energy storage systems. During the discharge process, Zn metal loses electrons and then reacts with OH<sup>-</sup>, generating the soluble Zn(OH)<sub>4</sub><sup>2-</sup> (Zn + 4OH<sup>-</sup> → Zn(OH)<sub>4</sub><sup>2-</sup> + 2e<sup>-</sup>). Subsequently, Zn(OH)<sub>4</sub><sup>2-</sup> would turn into insoluble ZnO (Zn(OH)<sub>4</sub><sup>2-</sup> → ZnO + 2OH<sup>-</sup> + H<sub>2</sub>O)

TABLE 1 Summary of Zn-metal-free anodes

Zn-metal-free anodes	Charge voltage (V vs. Zn/Zn <sup>2+</sup> )	Reversible capacity (mAh g <sup>-1</sup> )
H <sub>2</sub> Ti <sub>3</sub> O <sub>7</sub> ·xH <sub>2</sub> O <sup>28</sup>	~0.20	86.0
Mo <sub>6</sub> S <sub>8</sub> <sup>29,30</sup>	~0.35 ~0.65	88.0
Cu <sub>2-x</sub> Te <sup>31</sup>	~0.40	158.0
N <sub>a0.14</sub> TiS <sub>2</sub> <sup>32</sup>	~0.44	119.0
TiS <sub>2</sub> <sup>32</sup>	~0.55	133.0
9,10-AQ <sup>33</sup>	~0.60	173.1
Cu <sub>2-x</sub> Se <sup>31</sup>	~0.60	152.1
Hexagonal MoO <sub>3</sub> <sup>34</sup>	~0.63	120.0
PTCDI/rGO <sup>35</sup>	~0.75	138.0
Zn <sub>x</sub> Mo <sub>2.5+y</sub> VO <sub>9+z</sub> <sup>36</sup>	~0.90	220.0

and passivate electrodes when continually accumulated Zn(OH)<sub>4</sub><sup>2-</sup> become supersaturated. Reverse electrochemical and chemical reactions occur in the following charge procedure. However, daunting issues associated with dendrite growth, corrosion, passivation, and low Coulombic efficiency (CE) render poor cyclic stability and hold back their practical application.<sup>19</sup> To relieve these issues, researchers recently investigate Zn deposition/stripping behavior in mild acidic electrolytes (3.0 > pH > 6.0), that is, acidic ZMBs.<sup>20–22</sup> Compared with alkaline ZMBs, the formation of the ZnO passivation layer could be largely restrained in acidic counterparts due to the presence of H<sup>+</sup>, which improves deposition/stripping reversibility and inhibits dendrite growth to some extent. The working mechanism involves merely the reduction of Zn<sup>2+</sup>/oxidation of Zn metal. Considering these virtues, we mainly discuss acidic electrolyte-based ZMBs in this review.

Abundantly available cathode materials, such as manganese-based compounds, vanadium-based oxides, Prussian blue analogs, and organic compounds, have been developed with attractive electrochemical performance. For more information, readers can refer to many comprehensive review articles.<sup>23–27</sup> Several Zn-metal-free materials (e.g., insertion hosts) are proposed as the anodes to construct rock-chair type Zn-ion batteries that resemble LIBs. Nevertheless, the low cycling capacity (~130 mAh g<sup>-1</sup>) and relatively high charge voltage (~0.5 V vs. Zn/Zn<sup>2+</sup>) of these anodes significantly compromise the energy density of Zn-based batteries (literature summary in Table 1), making them uncompetitive with Zn metal anodes.<sup>37</sup> Consequently, intensive studies are conducted to resolve the dilemma of Zn metal anodes for constructing high-energy-density ZMBs.

## 2 | CHALLENGES OF ZINC METAL ANODES

Zn metal anodes are long afflicted by the Zn dendrite growth, HER and corrosion, and the corresponding by-products (Figure 2).<sup>38–40</sup> We will discuss the roots of the existing problems in this section and then demonstrate how the reported approaches to design advanced Zn metal anodes are closely related to these fundamental challenges.

### 2.1 | Mechanisms of dendrite growth

During the charge/discharge process of ZMBs, Zn deposition/stripping takes place on the anodes. The cycling performance of ZMBs is significantly related to Zn metal anodes' stability. Ideally, Zn metal anodes should remain smooth and compact morphologies even after long-term cycles, enabling the highly reversible ZMBs. However, non-uniform and loose Zn metal is generally formed during Zn deposition in practical scenarios due to the inhomogeneous electric field, Zn<sup>2+</sup> concentration distribution, etc. Such an uneven Zn deposition can be simplified as follows. Zn dendrite nucleation prefers to commence at electrode tips (i.e., “tip effect”) because both the Zn<sup>2+</sup> and electric field tend to concentrate at these positions with high surface energy,<sup>13,41</sup> which results in the inhomogeneous Zn deposition. What is worse, this preferential deposition behavior is a self-amplification process. Namely, the formed Zn protrusions further reinforce the electric field intensity and local Zn<sup>2+</sup> around them, which leads to the evolution of Zn protuberances into Zn dendrites upon cycling. With the growth direction of Zn dendrites perpendicular to the electrode, the continually growing dendrites would contact and easily pierce the separator because they have sharp tips/edges, submicron structure, and high Young's modulus (108 GPa), which physically bridges anode and cathode, causing a short circuit of ZMBs.

To reveal the dendrite formation mechanism, several models have been proposed based on the complementary theoretical and experimental results.<sup>42–45</sup> Among them, a space-charge model developed by Chazalviel in 1990 has been widely accepted to elucidate the dendrite initiation.<sup>42</sup> This model predicts that the dendrites start to appear when the cation concentration drops to zero near the electrode surface due to the formation of a large space charge and electric field. Sand's time ( $\tau$ ) is employed to describe the minimum time necessary for forming a space-charge field. Theoretically, it can be calculated using the following equation<sup>46,47</sup>:

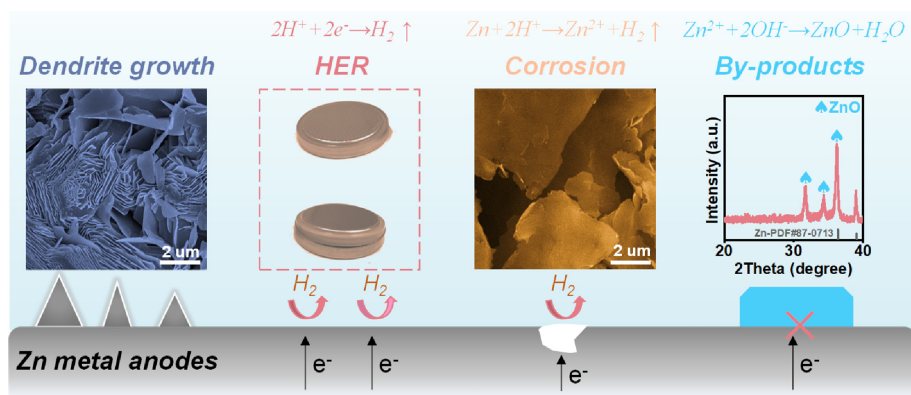


FIGURE 2 Illustration of the issues toward stable Zn metal anodes

$$\tau = \pi D \left( \frac{Z_c e C_o}{2J t_a} \right)^2 \quad (1)$$

where  $D$  is the diffusion coefficient,  $Z_c$  is the cationic charge number,  $e$  is the electronic charge,  $C_o$  is the bulk electrolyte concentration,  $t_a$  stands for the anionic transference number, and  $J$  presents the current density. This equation indicates decreasing  $J$  is beneficial to delaying the dendrite growth due to the inverse quadratic correlation between  $\tau$  and  $J$ . Note that the dendrite formation still appears even at a very small  $J$  due to the accumulated electric field on the electrode tips/lumps during the deposition process, resulting in the large local  $J$ . Thus, the reaction homogeneity also has a vital role in the deposition/stripping stability. Massive studies have focused on optimizing these factors for stable Zn metal anodes,<sup>48</sup> which will be elaborately discussed in the following dendrite suppression section.

## 2.2 | Fundamentals of HER and corrosion

Although aqueous media brings about unique advantages over organic ones, they give rise to HER and corrosion associated with water solvent (Figure 2). HER refers to the  $H^+$  electroreduction process, an electrochemical reaction ( $2H^+ + 2e^- \rightarrow H_2 \uparrow$ ). It takes place in the Zn deposition process, where  $H^+$  competes with  $Zn^{2+}$  to get the electrons. The resultant hydrogen gas would lead to a pressure upsurge inside the cells and cause safety concerns related to the swelling and rupture of cells. In addition, the generation of hydroxyl ions derived from HER brings about massive nonconductive by-products, for example, metal hydroxides/oxides, on Zn metal anodes. These side reactions consume the limited active Zn metal and electrolytes, resulting in a short cycle life. The challenges induced

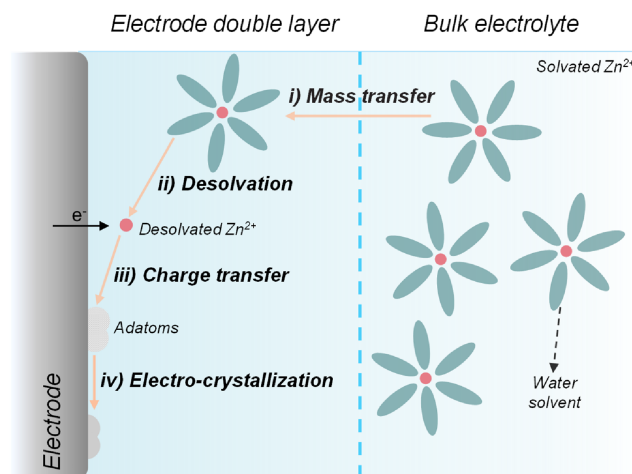
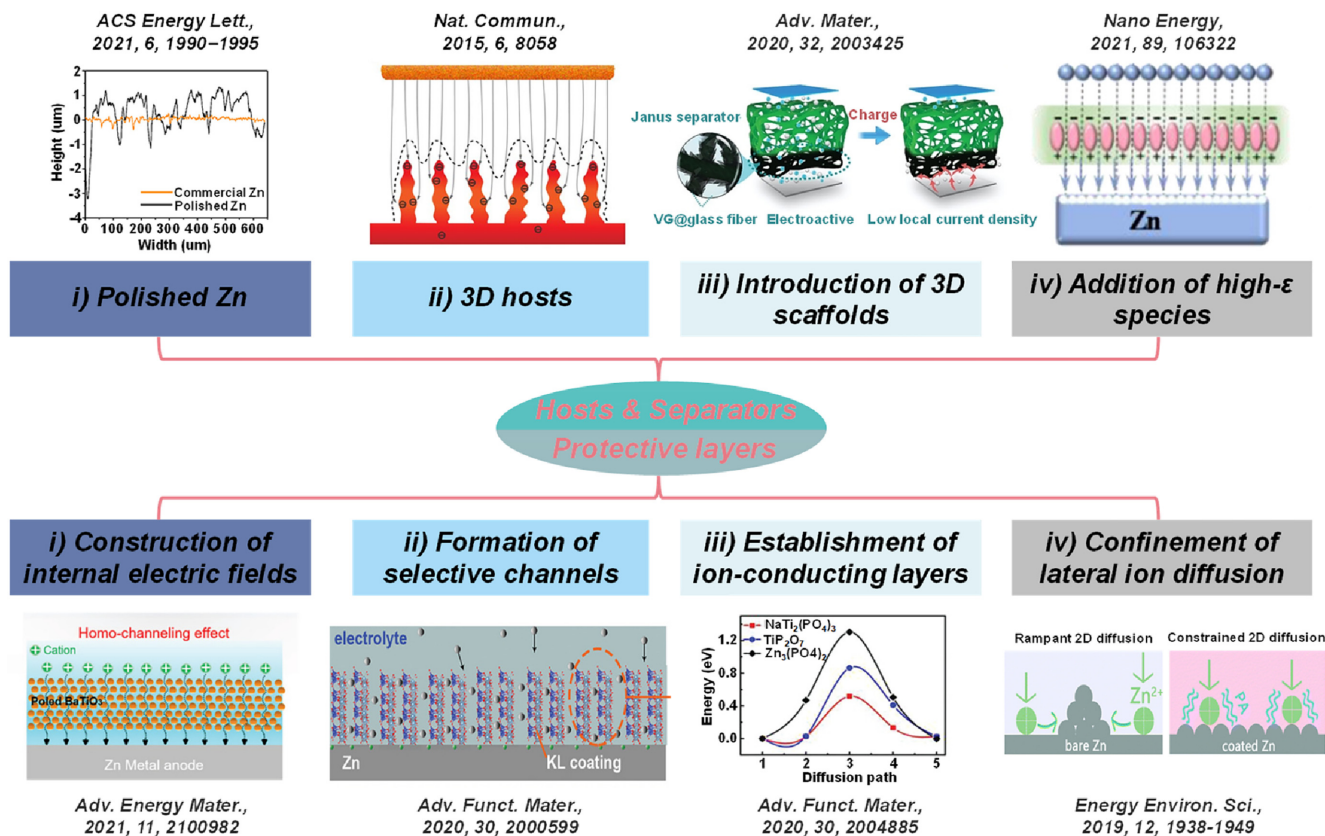


FIGURE 3 Illustration of the processes for electro-reducing  $Zn^{2+}$  into Zn metal

by the corrosion are basically the same as those of HER. Their main difference is that the corrosion is a chemical reaction (e.g.,  $Zn + 2H^+ \rightarrow Zn^{2+} + H_2 \uparrow$ ), making it occur even at a rest state in addition to the deposition process.

Theoretically, HER and corrosion are thermodynamically spontaneous processes in slightly acidic electrolytes due to the invariably lower reduction potential of  $Zn/Zn^{2+}$  than  $H_2/H^+$  (starts at 0 and  $-0.414$  V vs. SHE respectively at pH 0 and 7, see Figure 1D). Although the high kinetic overpotential of Zn metal for HER and corrosion slows down these side reaction rates, they do pose a great challenge to long-term stability.

It is worth mentioning that HER and corrosion aggravate the dendrite formation since the resultant by-products impede the homogeneity of  $Zn^{2+}$  transport and promote the dendrite initiation. In turn, as-formed dendrites with large surface areas facilitate these side reactions. Therefore, the above issues should be confronted concurrently, as they will resonate with each other to amplify the side effects.



**FIGURE 4** The working mechanisms and corresponding exemplifications of novel hosts, protective layers and separators. Reproduced with permission.<sup>52</sup> Copyright 2021, American Chemical Society, Reproduced with permission.<sup>55</sup> Copyright 2015, Nature Publishing Group, Reproduced with permission.<sup>79</sup> Copyright 2020, Wiley-VCH, Reproduced with permission.<sup>80</sup> Copyright 2021, Elsevier, Reproduced with permission.<sup>66</sup> Copyright 2021, Wiley-VCH, Reproduced with permission.<sup>69</sup> Copyright 2020, Wiley-VCH, Reproduced with permission.<sup>73</sup> Copyright 2020, Wiley-VCH and Reproduced with permission.<sup>76</sup> Copyright 2019, Royal Society of Chemistry

### 3 | ADVANCEMENTS IN DENDRITE SUPPRESSION STRATEGIES

To clearly elucidate the underlying working mechanisms of reported approaches, we separately summary and discuss the efforts to resolve dendrite growth and side reactions. It is well recognized that electro-reducing  $Zn^{2+}$  into Zn metal contains four successive steps (Figure 3)<sup>49-51</sup>: (i) Mass transfer:  $Zn^{2+}$  transport from the bulk electrolyte to the electrode surface through mass transfer, which involves three modes of migration, diffusion, and convection. (ii) Desolvation process:  $Zn^{2+}$  that are coordinated with six water molecules in aqueous electrolytes take off the partially/whole solvation sheath. (iii) Charge transfer: The partially/completely desolvated  $Zn^{2+}$  get electrons from the electrode to reduce into Zn adatoms. (iv) Electro-crystallization: The adatoms laterally diffuse along the electrode surface to form Zn clusters at energetically favorable sites. A set of approaches have been proposed by optimizing the above deposition processes to tackle

the dendrite growth problem. We classify the extensive efforts into four types corresponding to the four deposition steps, including  $Zn^{2+}$  flux regulation, desolvation process manipulation, charge transfer adjustment, and electro-crystallization control. Diverse approaches under each category are discussed in this section.

#### 3.1 | $Zn^{2+}$ flux regulation

$Zn^{2+}$  transport from the bulk electrolyte to the electrical double layer is the first step for Zn deposition. A uniform  $Zn^{2+}$  transport benefits the smooth Zn morphology. As the convection is negligible in sealed ZMBs, mass transport is dominated by migration and diffusion, driven by the electric field and concentration gradient, respectively. The homogeneous electric distribution and reduced concentration gradient on the electrode surface could inhibit the dendrite growth. Massive methods are established centered on these two working mechanisms (Figure 4).

### 3.1.1 | Polished Zn metal

Zn foils are commonly employed as anodes for ZMBs because they are readily manufactured. Many surface imperfections such as microcracks, scratches, and fold lines are inevitably introduced during Zn foils' manufacturing.<sup>52</sup> These defects bring about the uneven electric field distribution and Zn<sup>2+</sup> diffusion, leading to heterogeneous Zn nucleation and growth. The growth of dendrites can pierce the separator and cause a short circuit of ZMBs. Therefore, a smooth surface is desired for Zn foils. Many studies reprocess commercial Zn foils to minimize these defects and achieve morphological uniformity through simple approaches, such as physical and electrochemical polishing, resulting in a greatly improved electrochemical performance.<sup>53,54</sup> For instance, the sandpaper-polished Zn metal anode delivers a cycle life of ~800 h with over eightfold enhancement compared to the unpolished one at 1 mA cm<sup>-2</sup> for 1 mAh cm<sup>-2</sup>. Although the amelioration of these methods is commonly restricted at low current density and cycling capacity, it does provide a simple way to stabilize Zn metal anodes.<sup>52</sup> Combining with other strategies, polished Zn metal anodes could be further boosted. This research also highlights that researchers should make sure the performance improvements after modification not originated from the difference in initial Zn foils. To diminish the probability of this situation, the reproducible battery cyclic stability results for multicells are needed. In addition, a standardized polish procedure should be established and applied in current lab research to minimize the effect of different Zn foils on the electrochemical performance, hence benefiting the fair comparison among published works.

### 3.1.2 | Three-dimensional hosts

As mentioned above, the non-uniform electric field is easily formed on 2D Zn foils when there are imperfections on the surface. To solve this ubiquitous problem, three-dimensional (3D) hosts are developed because they have an open 3D porous skeleton than 2D ones.<sup>55</sup> Porous skeleton leads to homogeneous electric field distribution and Zn<sup>2+</sup> transport, which is beneficial to smooth Zn nucleation and growth.<sup>56</sup> In addition, Zn metal could be deposited into the pores of the 3D host, delaying surface deposition and dendrite growth. Another asset of 3D hosts is their larger surface area, which decreases practical current density for inhibiting dendrite formation. Thanks to these advantages, the 3D ridge-like Zn metal anode improves cycle life from 40 h for a 2D counterpart to 200 h.<sup>57</sup> In addition, various 3D current collectors, including metal- and carbon-based ones, are widely studied. They present an excellent potential for stabilizing Zn

metal anodes.<sup>58–62</sup> Both 3D Zn metal and current collectors are extensively studied, but their utilization for practical application is different. 3D Zn metal is directly employed as anodes, while Zn metal should be additionally electrodeposited on 3D current collectors, and these obtained current collectors are then applied as anodes.

Despite these advances, 3D architectures still suffer from many challenges. Due to the hindered Zn<sup>2+</sup> migration into the electrode bottom, Zn metal tends to deposit on 3D hosts' top surface instead of bottom/pores, especially at high current density and cycling capacity. Top-surface Zn deposition is more likely to pierce the separator and render a short circuit. This dilemma is partially resolved by a recent stratified deposition framework with three-layer geometry, realizing a bottom-to-top Zn deposition mode using their binding energy differences with Zn.<sup>63</sup> More efforts could be applied to develop practical and superior hierarchical 3D hosts. In addition, the high surface area of 3D hosts inevitably brings about an increased contact region between Zn metal and electrolytes, which in turn accelerates HER and corrosion. Thus, integrating an anti-corrosion strategy with 3D hosts is recommended. Another overlooked issue is related to the highly decreased energy and volumetric densities of ZMBs when heavy and thick 3D hosts are employed. Based on the above analyses, an excellent 3D structure for practical application should satisfy these requirements, that is, low cost, small thickness, lightweight, and enabling Zn bottom deposition.

### 3.1.3 | Protective layers

Protective layers play diversified roles in the Zn<sup>2+</sup> deposition process, such as regulating Zn<sup>2+</sup> flux<sup>64</sup> and optimizing the desolvation process of hydrated Zn<sup>2+</sup>.<sup>65</sup> In general, coating materials that can adjust Zn<sup>2+</sup> flux possess one of the following features: (i) Piezoelectricity generates an internal piezoelectric field, which boosts Zn<sup>2+</sup> mobility; (ii) A selective channel helps confine Zn<sup>2+</sup> diffusion; (iii) Fast ionic conductivity allows internal Zn<sup>2+</sup> transport; (iv) A strong interaction with Zn<sup>2+</sup> restrains 2D lateral diffusion of Zn<sup>2+</sup>. We discuss them separately as follows.

#### *Construction of internal electric fields*

The primary reason for dendrite formation is sluggish Zn<sup>2+</sup> transport, mainly controlled by electromigration and diffusion. Boosting Zn<sup>2+</sup> transport would delay the dendrite initiation and stabilize Zn metal anodes. With this in mind, internal fields, such as electric fields, are constructed to provide an additional driving force for Zn<sup>2+</sup> transport. For instance, polymer-BaTiO<sub>3</sub> coated Zn metal anode, in which BaTiO<sub>3</sub> ferroelectric species could create an internal electric field, help promote the Zn<sup>2+</sup> diffusion and realize a

smooth Zn deposition/stripping.<sup>66</sup> Such an internal electric field could be reinforced by an extra poling treatment on polymer-BaTiO<sub>3</sub> that immobilizes and maximizes the piezoelectricity capability of BaTiO<sub>3</sub> along its polarization direction, which further accelerates Zn<sup>2+</sup> transport and enables stable deposition/stripping at 10 mA cm<sup>-2</sup>. Despite the improved performance, thickness (15 μm) of the polymer-BaTiO<sub>3</sub> is too large, and thin coatings with a self-built internal field are needed for practical application.

#### *Formation of selective channels*

The introduction of protective layers with a selective channel can guide Zn<sup>2+</sup> diffusion pathways inside their pore structures, generating a specific ion-regulating effect.<sup>67,68</sup> For instance, kaolin (Al<sub>2</sub>Si<sub>2</sub>O<sub>5</sub>(OH)<sub>4</sub>), which possesses a selective channel of Zn<sup>2+</sup> and narrow distribution of pore diameter (~3.0 nm), is constructed on Zn metal as a protective layer to confine Zn<sup>2+</sup> migration.<sup>69</sup> Accordingly, such Zn metal anodes ensure uniform deposition and harvest a prolonged lifetime of 800 h. Similar functions are also observed using montmorillonite, where its interlayer serves as a freeway for Zn<sup>2+</sup> transport.<sup>70,71</sup> More efforts are necessitated to optimize the coating properties, such as channel size and coating thickness, for constructing ZMBs with long-term cyclic stability.

#### *Establishment of ion-conducting layers*

The ionic conductivity of protective layers plays a vital role in guiding uniform Zn diffusion. Many ion-conducting materials, such as NaTi<sub>2</sub>(PO<sub>4</sub>)<sub>3</sub> (NTP), hopeite (Zn<sub>3</sub>(PO<sub>4</sub>)<sub>2</sub>·4H<sub>2</sub>O) and ZnF<sub>2</sub>, have been developed as coatings to improve the Zn deposition/stripping reversibility.<sup>72-74</sup> For instance, NTP with fast ionic conductivity, as confirmed by theoretical calculation and cyclic voltammetry tests, is employed as an ion-conducting layer to allow internal mobility of Zn<sup>2+</sup>. It results in a homogeneous Zn<sup>2+</sup> flux for restraining dendrite formation.<sup>73</sup> Similarly, hopeite acting as a SEI possesses a high Zn<sup>2+</sup> transference number and Zn<sup>2+</sup> conductivity, enabling uniform and rapid Zn<sup>2+</sup> transport kinetics for dendrite-free Zn deposition.<sup>74</sup> At this stage, the reported Zn<sup>2+</sup>-conducting materials remain scarce.

#### *Confinement of lateral ion diffusion*

After Zn<sup>2+</sup> reaches the electrode surface, they would laterally diffuse along the surface to find energetically favorable sites for the following processes. Therefore, it is essential to restrict these preferential movements of Zn<sup>2+</sup> for uniform Zn deposition. To realize this goal, protective layers should exhibit strong interactions with Zn<sup>2+</sup>.<sup>75</sup> Taking polyamide (PA) as a typical example, its rich polar amide groups can strongly coordinate with Zn<sup>2+</sup> and offer an extra energy barrier for lateral movements of Zn<sup>2+</sup>, leading to increased nucleation seeds and dense Zn deposition.<sup>76</sup>

Analogous effects are also achieved in inorganic species, for example, ZnO with electrostatic attraction toward Zn<sup>2+</sup> and Zn-Sb<sub>3</sub>P<sub>2</sub>O<sub>14</sub> nanosheets showing a negative surface to adsorb the positive Zn<sup>2+</sup>.<sup>62,77</sup>

In short, these reported protective layers deliver a prolonged cycle life of Zn metal anodes due to the formation of uniform Zn<sup>2+</sup> flux through various working mechanisms. Nonetheless, most of them are too thick, with a thickness of ~20 μm. In terms of practical applications, it is promising to exploit nanothickness coatings without compromising electrochemical performance. The mechanical stability of protective layers should also be improved since the Zn metal anode undergoes severe volume swelling under a large cycling capacity.

### 3.1.4 | Novel separators

The separator serves as a vital component in ZMBs. It plays an essential role in Zn<sup>2+</sup> diffusion, but fewer studies focus on separator modification than other topics. At this stage, commercial glass fiber is commonly used as the separator due to its good compatibility with aqueous electrolytes, but the concentrated electric field on the uneven pores of glass fiber leads to a non-uniform electric field distribution.<sup>78</sup> Similar to the functions of 3D hosts, the introduction of 3D scaffolds on separators also helps construct a homogeneous electric field and lower local current density. Benefiting from these advantages, glass fiber modified by a 3D vertical graphene carpet enables smooth Zn<sup>2+</sup> transport and Zn deposition.<sup>79</sup> Besides extra coating on the surface, the component could also be integrated into the separator. For example, a composite separator that combines cellulose nanofibers and ZrO<sub>2</sub> is proposed to stabilize Zn metal anodes. ZrO<sub>2</sub> as a high dielectric constant species could generate the Maxwell-Wagner polarization effect, providing a directionally even electric field and accelerated Zn<sup>2+</sup> diffusion.<sup>80</sup> Qin et al. report an easy method to intrinsically circumvent the formation of the non-uniform electric field in glass fiber, that is, the employment of commercial filter membranes with uniform pore distribution.<sup>81</sup> Such a separator improves Zn metal anodes' lifetime from ~50 h for classical glass fiber to over 2600 h. In addition, functional groups are beneficial to guiding Zn<sup>2+</sup> flux for stable Zn metal anodes. This is proved by the polyacrylonitrile nanofiber separator with rich -CN, realizing excellent long-term durability over 1500 cycles in Zn/NH<sub>4</sub>V<sub>4</sub>O<sub>10</sub> full cells.<sup>82</sup> This impressive progress demonstrates that separator modification is a promising option for stabilizing Zn metal anodes. It merits more attention in future studies. Apart from the electric field and Zn<sup>2+</sup> flux regulation stated above, an ideal separator should possess high ionic conductivity,

high Young's modulus resisting Zn dendrites, decent flexibility, and good thermal stability.

### 3.1.5 | Electrostatic shield

It is well known that dendrite formation is a self-amplification process. Fundamental alteration of this deteriorative growth pattern could effectively delay dendrite formation, as proved by introducing some positive ions (e.g.,  $\text{Na}^+$  and  $\text{TBA}^+$ ) into electrolytes.<sup>83,84</sup> Specifically, these ions that have lower reduction potential than  $\text{Zn}^{2+}$  could adsorb in the tips and generate the electrostatic shield effect, avoiding continuous Zn deposition on these tips. This function is also observed after incorporating some organic additives into the electrolytes. They preferentially adsorb on the electrode's elevations rather than recesses, resulting in preferred  $\text{Zn}^{2+}$  reduction at concave for smooth Zn metal.<sup>85</sup> We note that the working mechanism of this method seems to be simple, but many crucial questions remain unclear and are urgent to be revealed. For instance, can we delicately adjust these additives' properties (e.g., charge density and ionic radius) to further enhance the performance? Whether all positive ions with a lower reduction potential than  $\text{Zn}^{2+}$  can benefit the Zn deposition/stripping stability?

### 3.1.6 | Cycling protocols

The commonly employed cycling protocol for ZMBs is charging/discharging at a constant current density between specific voltage ranges. In this manner, cation concentration would drop near the electrode surface due to sluggish ion diffusion as a rate-limiting step, leading to dendrite formation. The issue could be largely resolved by changing the current discharge/charge protocol. For instance, a pulsed cycling protocol, that is, 5/5 s (on/off), is proposed to allow the relaxation of an ion concentration gradient in the vicinity of the electrode.<sup>86</sup> Such conception highly suppresses Zn dendrite growth. Compared to other approaches, optimizing cycling protocols is straightforward without introducing additional procedures. However, a rare investigation is applied to this topic probably because it is challenging to combine them into the practical application of batteries. Future studies should focus on designing optimal cycling protocols for the minimum influences on the normal battery operation.

## 3.2 | Desolvation process manipulation

The desolvation process refers to solvated  $\text{Zn}^{2+}$  taking off their solvation sheaths before getting the electrons. The

process could be regulated by aforementioned protective layers<sup>65</sup> and electrolyte formulations.<sup>87</sup> Recently, Hou et al. examine the potential effect of desolvation kinetics on Zn deposition/stripping behavior by employing acetonitrile (AN) co-solvent as a model system.<sup>87</sup> The AN incorporation alters the solvation sheath from  $\text{Zn}(\text{H}_2\text{O})_6^{2+}$  to  $\text{Zn}(\text{H}_2\text{O})_3(\text{AN})_3^{2+}$  due to a stronger affinity between  $\text{Zn}^{2+}$  and AN (Figure 5A). As a result, this unique solvation structure elevates the desolvation energy barrier and nucleation overpotential (Figure 5B), resulting in supersaturation of adatoms accumulated on the electrode and the increased Zn nuclei. Such uniform Zn nucleation helps suppress Zn dendrite initiation and guides subsequent Zn deposition. A similar effect is also achieved in other organic co-solvents, such as dimethyl sulfoxide (DMSO).<sup>89</sup> It is worth noting that the slow desolvation kinetic inevitably renders an increased Zn deposition/stripping overpotential as well as a poor rate capability for many cathode materials due to the high desolvation energy.<sup>90</sup> Therefore, a balance between lifetime and polarization should be sought by optimizing the desolvation energy in future studies.

## 3.3 | Charge transfer adjustment

In comparison with mass transfer, charge transfer possesses a faster rate. This colossal speed discrepancy promotes  $\text{Zn}^{2+}$  depletion near electrode surface and Zn dendrite initiation. Theoretically, decreasing charge transfer speed could mitigate concentration polarization and Zn dendrite growth to a certain extent.<sup>91</sup> However, this has not yet been revealed in the community so far. One direct way to tune the charge transfer process is the alteration of the hosts' electrical conductivity, but it may induce other side effects such as large polarization. Rational experiment design is thus necessary to decouple the effect of electrical conductivity from other parameters.

In addition, the current density could determine the charge transfer rate: the higher it is, the faster the rate. Thus, higher current density ( $J$ ) is commonly considered to promote dendrite growth and lead to a shorter lifetime. However, such a relation is not always true, as evidenced by our recent study where the relative maximum stability is observed at a moderate current density due to its double-edged effects on the cyclic stability.<sup>88</sup> As shown in Figure 5C, besides the detrimental impact due to the reduced  $\tau$  ( $\tau \propto 1/J^2$ ), high  $J$  implies a fast nucleation rate ( $\nu_n, \nu_n \propto \exp(-(1/\log^2 J))$ ), which increases nucleation sites and contributes to enhanced stability. An initial high  $J$  (IHJ) cycling protocol is then proposed based on these discoveries. A high current density is applied for a short period to form sufficient nuclei at the initial stage, followed by cycling at a standard (low) current density



**FIGURE 5** Typical exemplifications of desolvation process, charge transfer and electro-crystallization manipulation. (A) Snapshots of the ab initio molecular dynamics simulations and (B) activation energies for hybrid water/AN electrolytes (HWAE-0 and HWAE-15, where the number denotes the volume percentage of AN in the solvent). Reproduced with permission.<sup>87</sup> Copyright 2020, Royal Society of Chemistry. (C) Theoretical correlation between  $\tau/\nu_n$  and  $J$ . (D) Voltage profile of IHJ model. Reproduced with permission.<sup>88</sup> Copyright 2022, Wiley-VCH. (E) Zn nucleation and deposition on zincophilic and zincophobic surfaces

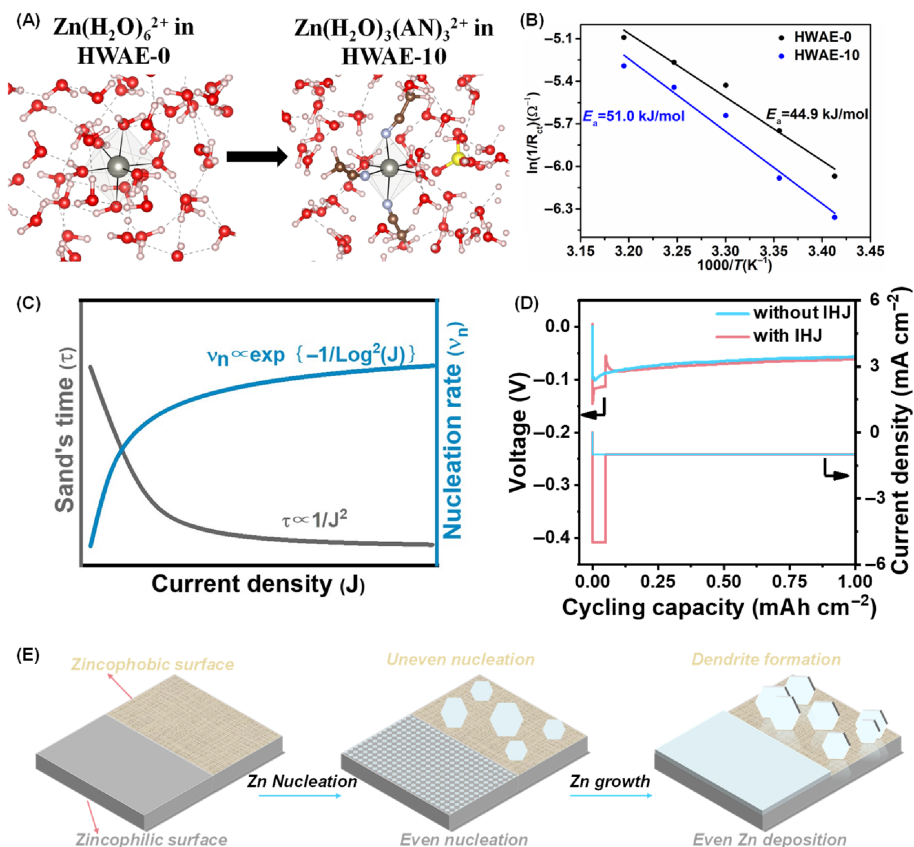


(Figure 5D), achieving highly stable Zn metal anodes without resorting to other modifications. This strategy could be readily extended to Li and K metal anodes.

### 3.4 | Electro-crystallization control

The last step for Zn deposition, the electro-crystallization process, refers to adatoms that diffuse along the electrode surface until they are adsorbed by the energetically favorable sites and then grow into clusters to form the deposit. This process is highly dependent on the electrode material properties. If adatoms can be incorporated close to where the initial adsorption occurred instead of the energetically favorable sites, abundant nucleation sites and subsequent smooth Zn deposition would be achieved. This hypothesis requires electrode materials to possess an excellent Zn affinity, giving rise to abundant active sites to accept adatoms incorporation (Figure 5E).<sup>92</sup> The term “zincophilicity”, as a similar concept of lithiophilicity in Li metal anodes, is used to describe the good Zn affinity of these electrode materials. For instance, zincophilic monolayer graphene with high lattice compatibility with Zn enables uniform distribution of Zn adatoms and stable Zn metal anodes.<sup>93,94</sup> Similarly, zincophilic metals, such as Au and In, are employed

for uniform Zn deposition/stripping.<sup>95,96</sup> A superior zincophilic material needs to meet the following requirements: (i) It is water-insoluble and electro-chemically stable during Zn deposition/stripping; (ii) It has a decent electric conductivity to transfer the electrons; (iii) It possesses a high kinetic overpotential for HER. In addition, it is better to combine these zincophilic species with 3D hosts to maintain zincophilic functions for the whole deposition process because zincophilic species in the 2D structure are easily covered by Zn metal during repeated Zn deposition/stripping.

Most available approaches concentrate on regulating the  $\text{Zn}^{2+}$  transport (i.e., first steps for Zn deposition) to improve Zn deposition/stripping (Table 2). The integration with other steps could further boost the stability. Although these reported approaches could partially address the Zn dendrite issues and stabilize ZMBs, most of them are still far away from the requirements of commercial applications. On the one hand, testing conditions are commonly limited to small current density and low cycling capacity. On the other hand, most sample modification processes are complicated and expensive, causing the abatement of low-cost merits for ZMBs. Thus, it is urgent to develop a more reliable and advanced method to achieve high-performance and high-availability Zn metal anodes simultaneously.

TABLE 2 Summary of electrochemical performance of previously reported works

Type	Modification method	Cycling capacity (mAh cm <sup>-2</sup> )	Current density (mA cm <sup>-2</sup> )	Cycle life (h)	Cumulative capacity (mAh cm <sup>-2</sup> )
Polished Zn metal	Sandpapers <sup>52,54</sup>	1	1	800	800
	Electropolishing <sup>53</sup>	2	40	600	24 000
3D hosts	Nanoporous Zn <sup>97</sup>	10	5	200	1000
	Carbon nanotube <sup>56</sup>	5	2.5	110	275
	Conductive graphite fiber <sup>60</sup>	1	1	700	700
	CNT scaffold <sup>58</sup>	0.5	0.1	1800	180
	Porous copper <sup>59</sup>	0.5	0.5	350	175
	Copper foam <sup>98</sup>	1	2	120	240
	Ti <sub>3</sub> C <sub>2</sub> T <sub>x</sub> MXene@Zn paper <sup>61</sup>	1	1	300	300
	Zn/stainless steel mesh composite <sup>99</sup>	2	1	300	300
	Ridge-like Zn <sup>57</sup>	1	0.5	200	100
	Stratified deposition framework <sup>63</sup>	3	4.5	250	1125
	Nanoporous Zn–Cu alloy <sup>97</sup>	–	2	300	600
	Zn@ZnO-3D <sup>62</sup>	1.25	5	500	2500
	Internal electric fields	PVDF/BaTiO <sub>3</sub> <sup>66</sup>	2	40	225
Selective channels	Kaolin <sup>69</sup>	1.1	4.4	800	3520
	Nafion/Zn-X zeolite <sup>100</sup>	1	10	1000	10 000
	PVDF/ZIF-7 <sup>101</sup>	0.5	0.5	3000	1500
	ZIF-8 <sup>102</sup>	10	10	400	4000
	Hydrogen-substituted graphdiyne <sup>103</sup>	0.1	2	2400	4800
	Stacked lamellar matrix <sup>68</sup>	7.1	14.2	180	2556
Ion-conducting layers	NaTi <sub>2</sub> (PO <sub>4</sub> ) <sub>3</sub> <sup>73</sup>	1	1	240	240
	ZnF <sub>2</sub> <sup>72</sup>	1	5	2500	12 500
	(Zn <sub>3</sub> (PO <sub>4</sub> ) <sub>2</sub> ·4H <sub>2</sub> O) <sup>74</sup>	1	5	200	1000
Confining lateral ion diffusion	Polyamide layer <sup>76</sup>	0.25	0.5	8000	4000
	ZnO <sup>62</sup>	1.25	5	500	2500
	Zn-Sb <sub>3</sub> P <sub>2</sub> O <sub>14</sub> nanosheets <sup>77</sup>	1	1	1300	1300
	Phytic acid <sup>75</sup>	2.5	5	1600	8000
Novel separators	Tin coated separator <sup>78</sup>	10	10	500	5000
	Vertical graphene carpet coated glass fiber <sup>79</sup>	1	10	600	6000
	Cellulose nanofibers-ZrO <sub>2</sub> composite separator <sup>80</sup>	2.5	5	1000	5000
	Filter membrane <sup>81</sup>	1	10	390	3900
Electrostatic shield effect	Na <sup>+</sup> additive <sup>84</sup>	–	–	–	–
	TBA <sup>+</sup> additive <sup>104</sup>	5	5	160	800
	Diethyl ether <sup>85</sup>	0.2	0.2	250	50
Cycling protocols	5/5 s (on/off) <sup>86</sup>	–	–	–	–
Desolvation kinetics	AN <sup>87</sup>	2	2	600	1200
	DMSO <sup>89</sup>	0.5	0.5	1000	500

TABLE 2 (Continued)

Type	Modification method	Cycling capacity (mAh cm <sup>-2</sup> )	Current density (mA cm <sup>-2</sup> )	Cycle life (h)	Cumulative capacity (mAh cm <sup>-2</sup> )
Charge transfer	IHJ <sup>88</sup>	1	1	2500	2500
Zincophilic hosts	Graphene substrates coated Zn <sup>93</sup>	–	–	–	–
	Au-coated Zn <sup>95</sup>	0.05	0.25	2000	500
	In-modified Zn <sup>96</sup>	1	1	500	500
	Ag-modified Zn <sup>105</sup>	–	–	–	–
HCE/LHCE	1 m Zn(TFSI) <sub>2</sub> + 20 m LiTFSI <sup>106</sup>	0.03	0.2	170	34
	30 m ZnCl <sub>2</sub> <sup>107</sup>	0.03	0.2	600	120
	0.5 m Zn(ClO <sub>4</sub> ) <sub>2</sub> + 18 m NaClO <sub>4</sub> <sup>108</sup>	0.02	0.2	1200	240
	Molten hydrate ZnCl <sub>2</sub> ·2.33H <sub>2</sub> O <sup>109</sup>	1	2	1000	2000
	1 m Zn(OAc) <sub>2</sub> + 31 m KOAc <sup>110</sup>	2	5	2000	10 000
	8 M NaClO <sub>4</sub> + 0.4 M Zn(CF <sub>3</sub> SO <sub>3</sub> ) <sub>2</sub> <sup>111</sup>	1	1	200	200
	1 m Zn(TFSI) <sub>2</sub> + 19 m LiTFSI + 9 m LiBETI-(water: 1,4 DX = 1:3 by molar) <sup>112</sup>	0.5	0.5	400	200
	Organic solvent-involved electrolytes	2 M ZnSO <sub>4</sub> -(H <sub>2</sub> O: methanol = 1:1 by volume) <sup>113</sup>	–	–	–
	2 M ZnSO <sub>4</sub> -(EG: H <sub>2</sub> O = 2:3 by volume) <sup>114</sup>	2	1	140	140
	2 M ZnSO <sub>4</sub> /(glycerol: water = 1:1) <sup>115</sup>	6	2	900	1800
	0.5 M Zn(CF <sub>3</sub> SO <sub>3</sub> ) <sub>2</sub> -TEP <sup>116</sup>	5	0.5	2000	1000
	0.5 M Zn(OTf) <sub>2</sub> -TMP <sup>117</sup>	10	1	1000	1000
	0.5 M Zn(OTf) <sub>2</sub> -(TEP: PC = 1:2) <sup>118</sup>	0.5	0.5	2500	1250
	0.5 M Zn(OTf) <sub>2</sub> -(TMP: DMC = 1:1 by volume) <sup>117</sup>	1	1	5000	5000
Adsorbed additives	Sodium dodecyl benzene sulfonate <sup>119</sup>	–	0.5	1500	750
	Polyethylene oxide <sup>120</sup>	–	–	–	–
	Polyacrylamide <sup>121</sup>	4	2	280	560
In situ protective layers	ZnF <sub>2</sub> and organic components <sup>122</sup>	0.5	1	100	100
	ZnF <sub>2</sub> and ZnCO <sub>3</sub> <sup>123</sup>	2.5	5	800	4000
	Zn <sub>3</sub> (PO <sub>4</sub> ) <sub>2</sub> and ZnF <sub>2</sub> <sup>65</sup>	20	10	250	2500
	Cl <sup>-</sup> containing layer <sup>124</sup>	1	1	3000	3000
Ex situ protective layers	PVB <sup>125</sup>	0.5	0.5	2200	1100
	Sc <sub>2</sub> O <sub>3</sub> <sup>126</sup>	2	2	240	480
	PVDF/TiO <sub>2</sub> <sup>127</sup>	8.85	8.85	250	2212.5
Electrode activity regulation	Cu/Zn layer-modified Zn <sup>128</sup>	0.5	1	1500	1500
	PEG <sup>129</sup>	–	–	–	–

Notes: The cumulative capacity is calculated by multiplying current density and cycle life.

## 4 | ADVANCEMENTS IN HER AND CORROSION INHIBITION STRATEGIES

Undesired HER and corrosion render poor CE and short cycle life. Approaches to suppress them are commonly overlapped because both HER and corrosion are related to water media. Therefore, we discuss them together in this section. The working mechanisms include reducing water content in the solvation structure, isolating electrode and electrolyte, and decreasing electrode activity. Accordingly, current research is divided into three categories, that is, solvation structure regulation, interface control, and electrode activity modification.

### 4.1 | Solvation structure regulation

As discussed before, the desolvation process is one of the steps for Zn deposition. Water molecules released from solvated  $\text{Zn}^{2+}$  in the desolvation process have weakened H–O bonds than water molecules in bulk electrolytes.<sup>39</sup> Namely, these more active water molecules easily change into  $\text{H}^+$ , which then compete with  $\text{Zn}^{2+}$  to be reduced into  $\text{H}_2$ . Therefore, decreasing water molecule contents in the solvation structure helps decrease the electrochemically reactive water, suppressing HER. In addition, massive free water molecules exist in the traditional dilute electrolyte, potentially posing a risk to stable Zn metal anodes. If these free water molecules are confined, both HER and corrosion can be restrained.<sup>130</sup> Thus, extensive studies are devoted to optimizing electrolyte solvation structure.

#### 4.1.1 | (Localized) high-concentration electrolytes

Recently, high-concentration electrolytes (HCE) have been proposed to reduce HER and corrosion to improve electrochemical performance. The presence of massive salts shifts water molecule-occupied solvation sheaths to anion-occupied ones and changes free water molecules into fixed ones. One of the typical examples is the electrolyte of 1 M  $\text{Zn}(\text{TFSI})_2 + 20 \text{ M LiTFSI}$  (Figure 6A), which enables smooth Zn deposition/stripping at  $\sim 99.7\%$  CE.<sup>106</sup> The main drawbacks of HCE are the high cost and viscosity, hindering their large-scale application, and the fast discharge/charge rates. This dilemma is partly solved through introducing the low-solvating organic solvents into HCE to form localized high-concentration electrolytes (LHCE). For instance, 1,4-dioxane is reported to be a diluent and a hydrogen bond modulator, addressing

HCE' issues related to the cost, viscosity, conductivity, wettability, etc.<sup>112</sup> There remain many roadblocks for LHCE. A suitable diluent should have the following features: (i) It is a non-polar solvent that cannot dissociate salts and should be miscible with water; (ii) It is nonflammable; (iii) It has low cost and viscosity. Up to now, such a solvent has not yet been fully developed to dilute HCE in ZMBs.

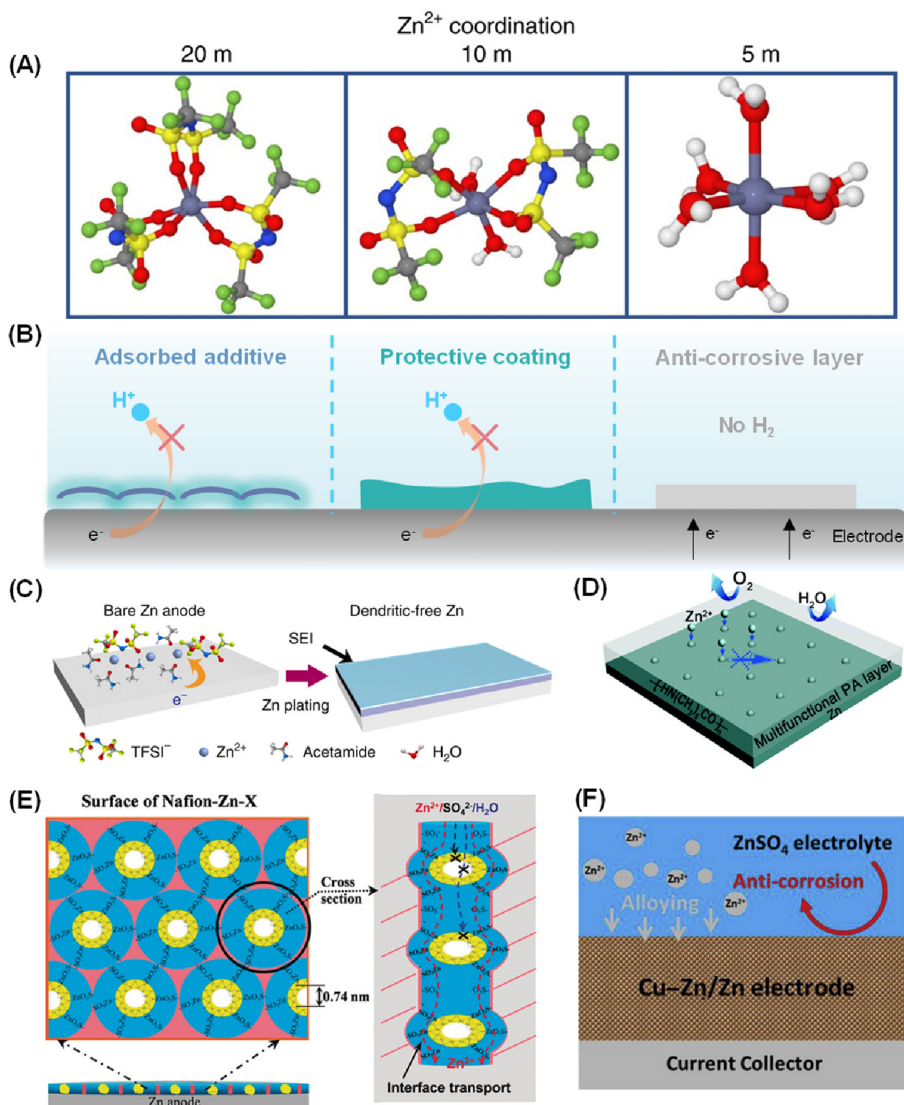
#### 4.1.2 | Organic solvent-involved electrolytes

Apart from increasing salts' concentration to inhibit side reactions, organic solvents with similar functions emerge to tune the solvation structure. Because of their high polarity, such solvents can replace water molecules in the solvation structure and reduce water activity by breaking the water–water hydrogen bonds as well as forming the hydrogen bonds with water.<sup>113</sup> For example, the adoption of oligomer poly(ethylene glycol) dimethyl ether as a competitive solvent in the electrolytes enables the alternative solvation sheath and the preferential surface adsorption, realizing wide-temperature Zn metal anodes.<sup>131</sup> These improvements are at the cost of safety due to the flammable organic solvents employed. To avoid this concession, nonflammable solvents with similar functions, for example, triethyl phosphate, are adopted to stabilize Zn metal anodes.<sup>116</sup> Despite the reduced water molecule contents in the solvation structure and the suppressed water activity in these hybrid electrolytes, water-induced HER and corrosion still exist. To completely eliminate these side reactions, pure organic solvent-based electrolytes, such as 0.5 M  $\text{Zn}(\text{OTf})_2$  in trimethyl phosphate, are exploited, showing enhanced cycling stability for over 2000 h.<sup>117</sup> These observations indicate the utilization of aqueous/non-aqueous or non-aqueous solvents is effective in restricting the side reactions, but they inevitably compromise water's superiority in the low cost and fast ionic diffusion. Therefore, the percentage of organic solvent additive in the electrolyte should be minimized to maintain the advantages of aqueous electrolytes while enhancing the reliability.

### 4.2 | Interface control

The water solvent participates in both HER and corrosion reactions. If we can effectively isolate the electrode and electrolyte, these side reactions would be restrained significantly. The frequently used approaches are the addition of adsorbed additives and the construction of protective layers (Figure 6B).

**FIGURE 6** Solvation structure, interface and electrode activity control. (A) Representative  $\text{Zn}^{2+}$ -solvation structures in the electrolytes with 1 m Zn(TFSI)<sub>2</sub> and LiTFSI with three different concentrations of 5, 10, and 20 m. Reproduced with permission.<sup>106</sup> Copyright 2018, Nature Publishing Group. (B) Schematic of working mechanisms for interface control and electrode activity modification to suppress side reactions. (C) The formation of SEI for Zn metal anode in acetamide-Zn(TFSI)<sub>2</sub> eutectic electrolyte. Reproduced with permission.<sup>122</sup> Copyright 2019, Nature Publishing Group. (D) The PA coating inhibits the permeation of O<sub>2</sub> and H<sub>2</sub>O. Reproduced with permission.<sup>76</sup> Copyright 2019, Royal Society of Chemistry. (E)  $\text{Zn}^{2+}$  transport mechanisms in Nafion-Zn-X protective layer. Reproduced with permission.<sup>100</sup> Copyright 2020, Wiley-VCH. (F) Schematic illustration of the role of the Cu-Zn alloy on the Cu-Zn/Zn electrode. Reproduced with permission.<sup>128</sup> Copyright 2020, Elsevier



#### 4.2.1 | Adsorbed additives

Several additives are proposed to stabilize Zn metal anodes as they are preferentially adsorbed on the electrode surface to obtain low interfacial energy. Surfactants, for example, sodium dodecylbenzene sulfonate, show a substantial blocking effect in shielding Zn metal anodes.<sup>119</sup> Surfactants have hydrophilic and hydrophobic groups, exposing the latter to the electrolyte to prevent the contact between the electrode and water. Similar functions are also observed by adding polyacrylamide, polyethylene oxide, etc.<sup>122,123</sup> Knowing that these adsorbed additives are helpful, many critical questions remain obscure. Can we modify the hydrophilic and hydrophobic groups of surfactants to manipulate and improve their effectiveness? What is the most critical parameter determining the functions of these additives? It is necessary to further investigate their working mechanisms to screen the superior additives.

#### 4.2.2 | In situ protective layers

In Li metal batteries, a passivating film, that is, solid electrolyte interphase (SEI), is spontaneously formed on Li metal anodes when Li metal contacts electrolytes. This SEI, which has excellent ionic conductivity and is electrically insulating, could effectively prevent further side reactions between the electrodes and electrolytes. Turning to Zn metal anodes, SEI is challenging to be in situ formed in aqueous electrolytes because the decomposition of water leads to H<sub>2</sub> and ionically insulating by-products with loose structures. Additionally, the electrochemical reduction of salts is almost impossible due to their lower reduction potential than Zn<sup>2+</sup> deposition. Therefore, electrolyte composition regulation is proposed to generate a stable SEI for Zn metal anodes. Acetamide-Zn(TFSI)<sub>2</sub> eutectic electrolyte is reported to construct a SEI with ZnF<sub>2</sub> and Zn<sup>2+</sup>-permeable organic components (Figure 6C), which originates from the preferential reductive decomposition of anion prior to Zn deposition in

anion-containing Zn complexes.<sup>122</sup> Similarly, organic solvents, for example, dimethyl carbonate, are introduced into aqueous electrolytes to form an organic molecule/anion-involved solvation structure, which contributes to the formation of a robust ZnF<sub>2</sub> and ZnCO<sub>3</sub>-rich SEI.<sup>123</sup> Although the formation of these SEIs greatly mitigates the side reactions, the existence of organic solvents in the aqueous electrolyte is inevitably detrimental to the merits of water solvents. This encourages researchers to develop SEI in pure water-based electrolytes. Encouragingly, a successful example has been demonstrated recently in the Zn(ClO<sub>4</sub>)<sub>2</sub>-water electrolyte. It is proposed that ClO<sub>4</sub><sup>-</sup> could be reduced into Cl<sup>-</sup> containing layer serving as a SEI.<sup>124</sup> At this stage, a few in-situ SEIs have been prepared on Zn metal anodes to suppress side reactions through altering electrolyte formulations. However, many vital questions remain ambiguous. Can we precisely manipulate SEI compositions on Zn metal anodes by simply altering electrolyte components, just like in lithium metal anodes cases (e.g., fluoroethylene carbonate additives induces the formation of LiF-rich SEI<sup>132</sup>)? How do these SEI species transport Zn<sup>2+</sup>? Revealing these critical puzzles is beneficial to boosting the development of SEI for aqueous Zn metal anodes.

### 4.2.3 | Ex situ protective layers

The construction of ex situ protective coatings onto electrodes is another way to separate the electrode and electrolyte. Compared to the in situ coatings, ex situ ones possess precise and facile control advantages. Solid polymer materials, such as PA and polyvinyl butyral, are widely used to serve as artificial SEIs (Figure 6D).<sup>76,125</sup> Analogously, many inorganic materials are exploited as protective layers. ZnF<sub>2</sub>, TiO<sub>2</sub>, Sc<sub>2</sub>O<sub>3</sub>, and kaolin are good illustrations.<sup>72,126,127</sup> Although both organic and inorganic coatings could decrease side reactions, the contact between Zn metal and electrolyte still exists because they are hydrophilic to guarantee Zn<sup>2+</sup> diffusion. Hybrid coatings are likely to resolve this issue, confirmed by the Nafion-Zn-X coating, including organic Nafion and inorganic Zn-X zeolite nanoparticles.<sup>100</sup> Their combination intelligently allows only bare Zn<sup>2+</sup> transport but prohibits water and anions (Figure 6E). Similarly, benefiting from their ordered nanopores to tune the solvation state of Zn<sup>2+</sup>, MOF-based materials could reduce HER and corrosion. For example, when solvated Zn<sup>2+</sup> across ZIF-7 coating, it compels solvated Zn<sup>2+</sup> to remove their solvation sheath due to the smaller pore size (2.94 Å) of ZIF-7 than solvated Zn<sup>2+</sup>.<sup>101</sup> This dramatically helps decrease contact between the electrode and water-occupied solvation sheath. We summarize the required properties for a decent protective layer: including (i) it should be hydrophilic but has massive nano-channels for merely bare

Zn<sup>2+</sup> diffusion; and (ii) it should also be uniform in composition for preventing preferential deposition, which is not well considered in most reported studies.

## 4.3 | Electrode activity modification

Electrode material plays a vital role in determining the rate of HER and corrosion. For instance, pure Zn metal suffers from a large corrosion current of 37.15 uA cm<sup>-2</sup>, while introducing anti-corrosive Cu metal to form Cu/Zn layer-modified Zn metal endows an improved anti-corrosive ability, showing a low corrosion current of 6.03 uA cm<sup>-2</sup> (Figure 6F).<sup>128</sup> Similarly, the indium (In) layer prepared on Zn metal anodes could restrain both HER and corrosion due to its high kinetic overpotential and good chemical inactivity.<sup>96</sup> However, there is a problem that has not been well considered. Zn metal is likely to deposit on these top modified layers during Zn deposition because they are conductive. Once they are fully covered by deposited Zn metal, they would suffer from a failure. It is promising to uniformly integrate these effective elements with Zn elements into a Zn metal composite rather than on a Zn metal surface to circumvent the challenge. In this way, these elements would continually maintain their functions. Note that the utilization of these composite anodes would introduce inactive materials and decrease the energy density. Therefore, it is necessary to optimize introduced species and their contents in composite anodes. Apart from introducing exotic elements, crystallographic orientation regulation is developed to suppress side reactions via the employment of organic additives. For instance, polyethylene glycol (PEG) additive enables increased (002) and (103) crystal planes of deposited Zn metals, exhibiting a reduced corrosion rate.<sup>129</sup>

In short, HER and corrosion could be inhibited from different perspectives, but most reported approaches are accomplished at the expense of cost, safety, and energy density. Furthermore, current research mainly focuses on kinetic control to decrease the speeds of side reactions but cannot eliminate them. If we can develop methods from thermodynamic aspects, it is hopeful to fully solve these issues.

## 5 | SUMMARY AND OUTLOOK

In conclusion, ZMBs have recently received massive attention as a promising large-scale EES system due to their unique advantages on safety, cost, and environmental friendliness. Extensive efforts have been dedicated to screening and developing appropriate cathode materials,

mainly including manganese-based compounds, vanadium-based oxides, Prussian blue analogs, and organic compounds. Further investigations are required to disclose the detailed storage mechanisms of these cathode materials (e.g., manganese dioxide),<sup>133</sup> and boost the reversible capacity, working voltage and long-term stability.<sup>10,27</sup> Turning to anode side, their commercial application is highly plagued by several intractable issues, including dendrite growth, HER, and corrosion, which significantly hold back their practical application. In response to these challenges, tremendous approaches have been developed. The Zn deposition involves mass transfer, desolvation, charge transfer, and electro-crystallization. Correspondingly, the efforts to deal with dendrite growth are divided into four classifications, including Zn<sup>2+</sup> flux regulation, desolvation process manipulation, charge transfer adjustment, and electro-crystallization control. Among them, a maximum of interest is dedicated to regulating mass transfer. More investigations are necessary for optimizing other steps. Regarding side reactions suppression, the proposed methods fall into three parts, that is, solvation structure regulation, interface control, and electrode activity modification.

Although impressive breakthroughs have been achieved with these substantial investigations, the impractical testing parameters at a lab-scale, such as superfluous electrolytes and large excess Zn metal amount, make them hard to transfer to the commercial application directly. Besides, the fundamental understandings are still at the developing stage, and many crucial questions remain ambiguous. The perspective and research directions for future studies are proposed as follows.

a. Establishing standardized testing conditions. Apart from current density and cycling capacity that can highly affect the stability of Zn metal anode,<sup>88</sup> other factors, for example, depth of discharge (DOD), electrolyte amount, and thickness of Zn metal, also have a substantial impact on Zn deposition/stripping process. These parameters greatly determine the energy density of Zn metal anodes. For instance, the practical capacity of Zn metal anodes is calculated by multiplying its theoretical capacity (820 mAh g<sup>-1</sup>) and the DOD. At this stage, the DOD of most research is lower than 10%. Namely, Zn metal anodes deliver a lower capacity of 82 mAh g<sup>-1</sup>, which dramatically reduces the energy density of ZMBs. Therefore, it is necessary to clearly state the effect of these critical parameters on Zn deposition/stripping lifetime and find the optimal balance between them. Moreover, a standard parameter setting should be established and applied for lab tests to propel the commercial application of ZMBs.

- b. All-embracing strategy. We separately discuss the modified method for dendrite growth and side reactions for straightforward elucidation. Commercial application of ZMBs is only possible if these challenges are overcome concurrently. It suggests that the proposed strategies should be reasonably integrated to realize advanced Zn metal anodes. For example, the methods of electrolyte formulation optimization and protective layer engineering are likely to be combined for constructing an omnipotent Zn metal anode. However, there have rarely been demonstrations of such combined modifications. It remains unclear how to incorporate these different approaches efficiently.
- c. Advanced characterization techniques. Although exciting progress achieved via diverse methods, their underlying mechanisms are difficult to be fully revealed under ex situ analytical techniques. This urgently stimulates researchers to develop new operando analytical techniques that allow accurate probing of failure patterns of batteries and working mechanisms of as-proposed strategies. For example, operando transmission electron microscopy (TEM) in a liquid environment could be employed to observe the Zn initial nucleation on zincophilic and zincophobic substances. It can be a powerful tool to clearly identify how zincophilicity influences the nucleation density and then provide fresh insight for rationally seeking/designing zincophilic materials. The recent study by Sasaki's group, which visualizes the Zn deposition/growth in nanoscale by in-situ TEM, has demonstrated the great potential of this promising direction.<sup>134</sup>
- d. Battery health monitoring. Health monitoring is essential for ZMBs since they would be employed for large-scale EES that demand an in-service lifetime of at least 20 years.<sup>135</sup> A lesson could be learned from the LIBs, where extensive healthy monitor techniques have been developed.<sup>136,137</sup> The most recent invention implants an optical fiber into the commercial 18 650 cells to track the gas generation and temperature variation,<sup>138,139</sup> which could be adopted in ZMBs. However, implementing real-time monitoring without significantly increasing costs remains challenging.
- e. Electrode remedy. Almost all of the research aim to suppress dendrite growth, but the formation of Zn dendrites is inherently unavoidable, notably at rigorous testing conditions, since such a process is thermodynamically and kinetically favorable. The tactics that can in situ eliminate the formed dendrites are thus urgently needed. Encouragingly, a tin (Sn) coated separator is recently proposed to control dendrite growth.<sup>78</sup> On the one hand, the conductive Sn coating dramatically homogenizes the electric field distribution for uniform Zn deposition. On the other hand, its

excellent zincophilicity triggers the concurrent deposition of Zn on both the separator and the substrate with a face-to-face growth, eliminating the inevitably formed Zn dendrites. Thanks to these synergetic effects, superior cycling stability is achieved at simultaneous high current densities and large cycling capacities. In addition, an advanced cycling protocol containing a low current density is also developed to eradicate already-formed dendrites.<sup>140</sup> More self-healing methodologies need to be exploited to in situ remedy in-service batteries to increase the lifespan.

## ACKNOWLEDGMENTS

This work was supported by the General Research Fund (GRF) scheme of the Hong Kong Research Grants Council (project no. 15307221).

## CONFLICT OF INTEREST

The authors declare no conflict of interest.

## ORCID

Biao Zhang  <https://orcid.org/0000-0001-8687-8946>

## REFERENCES

- Poizot P, Dolhem F. Clean energy new deal for a sustainable world: from non-CO<sub>2</sub> generating energy sources to greener electrochemical storage devices. *Energy Environ Sci.* 2011;4(6):2003-2019.
- Kittner N, Lill F, Kammen DM. Energy storage deployment and innovation for the clean energy transition. *Nat Energy.* 2017;2(9):1-6.
- Armand M, Tarascon J-M. Building better batteries. *Nature.* 2008;451(7179):652-657.
- Xu K. Electrolytes and interphases in Li-ion batteries and beyond. *Chem Rev.* 2014;114(23):11503-11618.
- Tarascon J-M, Armand M. Issues and challenges facing rechargeable lithium batteries. *Nature.* 2011;414(6861):359-367.
- Liu Z, Qin L, Lu B, Wu X, Liang S, Zhou J. Issues and opportunities facing aqueous Mn<sup>2+</sup>/MnO<sub>2</sub>-based batteries. *ChemSusChem.* 2022;15(10):e202200348.
- Chao D, Zhou W, Xie F, et al. Roadmap for advanced aqueous batteries: from design of materials to applications. *Sci Adv.* 2020;6(21):eaba4098.
- Bin D, Wang F, Tamirat AG, et al. Progress in aqueous rechargeable sodium-ion batteries. *Adv Energy Mater.* 2018;8(17):1703008.
- Pan Z, Liu X, Yang J, et al. Aqueous rechargeable multivalent metal-ion batteries: advances and challenges. *Adv Energy Mater.* 2021;11(24):2100608.
- Ruan P, Liang S, Lu B, Fan HJ, Zhou J. Design strategies for high-energy-density aqueous zinc batteries. *Angew Chem Int Ed.* 2022;61(17):e202200598.
- Quaino P, Juarez F, Santos E, Schmickler W. Volcano plots in hydrogen electrocatalysis—uses and abuses. *Beilstein J Nanotechnol.* 2014;5(1):846-854.
- Yuan L, Hao J, Kao C-C, et al. Regulation methods for the Zn/electrolyte interphase and the effectiveness evaluation in aqueous Zn-ion batteries. *Energy Environ Sci.* 2021;14(11):5669-5689.
- Yang Q, Li Q, Liu Z, et al. Dendrites in Zn-based batteries. *Adv Mater.* 2020;32(48):2001854.
- Hao J, Li X, Zeng X, Li D, Mao J, Guo Z. Deeply understanding the Zn anode behaviour and corresponding improvement strategies in different aqueous Zn-based batteries. *Energy Environ Sci.* 2020;13(11):3917-3949.
- Hawley WB, Li J. Electrode manufacturing for lithium-ion batteries—analysis of current and next generation processing. *J Energy Storage.* 2019;25:100862.
- Bayaguud A, Fu Y, Zhu C. Interfacial parasitic reactions of zinc anodes in zinc ion batteries: underestimated corrosion and hydrogen evolution reactions and their suppression strategies. *J Energy Chem.* 2022;64:246-262.
- Verma V, Kumar S, Manalastas W, Srinivasan M. Undesired reactions in aqueous rechargeable zinc ion batteries. *ACS Energy Lett.* 2021;6(5):1773-1785.
- Han C, Li W, Liu HK, Dou S, Wang J. Principles and strategies for constructing a highly reversible zinc metal anode in aqueous batteries. *Nano Energy.* 2020;74:104880.
- Parker JF, Chervin CN, Pala IR, et al. Rechargeable nickel-3D zinc batteries: an energy-dense, safer alternative to lithium-ion. *Science.* 2017;356(6336):415-418.
- Lu W, Zhang C, Zhang H, Li X. Anode for zinc-based batteries: challenges, strategies, and prospects. *ACS Energy Lett.* 2021;6(8):2765-2785.
- Yi Z, Chen G, Hou F, Wang L, Liang J. Strategies for the stabilization of Zn metal anodes for Zn-ion batteries. *Adv Energy Mater.* 2020;11(1):2003065.
- Zhang Q, Luan J, Tang Y, Ji X, Wang H. Interfacial design of dendrite-free zinc anodes for aqueous zinc-ion batteries. *Angew Chem Int Ed.* 2020;59(32):13180-13191.
- Yong B, Ma D, Wang Y, Mi H, He C, Zhang P. Understanding the design principles of advanced aqueous zinc-ion battery cathodes: from transport kinetics to structural engineering, and future perspectives. *Adv Energy Mater.* 2020;10(45):2002354.
- Fang G, Zhou J, Pan A, Liang S. Recent advances in aqueous zinc-ion batteries. *ACS Energy Lett.* 2018;3(10):2480-2501.
- Song M, Tan H, Chao D, Fan HJ. Recent advances in Zn-ion batteries. *Adv Funct Mater.* 2018;28(41):1802564.
- Wan F, Zhou X, Lu Y, Niu Z, Chen J. Energy storage chemistry in aqueous zinc metal batteries. *ACS Energy Lett.* 2020;5(11):3569-3590.
- Liu H, Wang J-G, You Z, Wei C, Kang F, Wei B. Rechargeable aqueous zinc-ion batteries: mechanism, design strategies and future perspectives. *Mater Today.* 2021;42:73-98.
- Liu Y, Zhou X, Wang X, et al. Hydrated titanate as an ultralow-potential anode for aqueous zinc-ion full batteries. *Chem Eng J.* 2021;420:129629.
- Chae MS, Heo JW, Lim SC, Hong ST. Electrochemical zinc-ion intercalation properties and crystal structures of ZnMo<sub>6</sub>S<sub>8</sub> and Zn<sub>2</sub>Mo<sub>6</sub>S<sub>8</sub> chevrel phases in aqueous electrolytes. *Inorg Chem.* 2016;55(7):3294-3301.
- Cheng Y, Luo L, Zhong L, et al. Highly reversible zinc-ion intercalation into chevrel phase Mo<sub>6</sub>S<sub>8</sub> nanocubes and applications for advanced zinc-ion batteries. *ACS Appl Mater Interfaces.* 2016;8(22):13673-13677.



31. Yang Y, Xiao J, Cai J, et al. Mixed-valence copper selenide as an anode for ultralong lifespan rocking-chair Zn-ion batteries: an insight into its intercalation/extraction kinetics and charge storage mechanism. *Adv Funct Mater.* 2020;31(3):2005092.
32. Li W, Wang K, Cheng S, Jiang K. An ultrastable presodiated titanium disulfide anode for aqueous “rocking-chair” zinc ion battery. *Adv Energy Mater.* 2019;9(27):1900993.
33. Yan L, Zeng X, Li Z, et al. An innovation: dendrite free quinone paired with  $ZnMn_2O_4$  for zinc ion storage. *Mater Today Energy.* 2019;13:323-330.
34. Xiong T, Zhang Y, Wang Y, Lee WSV, Xue J. Hexagonal  $MoO_3$  as a zinc intercalation anode towards zinc metal-free zinc-ion batteries. *J Mater Chem A.* 2020;8(18):9006-9012.
35. Liu N, Wu X, Zhang Y, et al. Building high rate capability and ultrastable dendrite-free organic anode for rechargeable aqueous zinc batteries. *Adv Sci.* 2020;7(14):2000146.
36. Kaveevivitchai W, Manthiram A. High-capacity zinc-ion storage in an open-tunnel oxide for aqueous and nonaqueous Zn-ion batteries. *J Mater Chem A.* 2016;4(48):18737-18741.
37. Tian Y, An Y, Wei C, et al. Recent advances and perspectives of Zn-metal free “rocking-chair”-type Zn-ion batteries. *Adv Energy Mater.* 2020;11(5):2002529.
38. Du W, Ang EH, Yang Y, Zhang Y, Ye M, Li CC. Challenges in the material and structural design of zinc anode towards high-performance aqueous zinc-ion batteries. *Energy Environ Sci.* 2020;13(10):3330-3360.
39. Li M, Li Z, Wang X, et al. Comprehensive understanding of the roles of water molecules in aqueous Zn-ion batteries: from electrolytes to electrode materials. *Energy Environ Sci.* 2021;14(7):3796-3839.
40. Jia H, Wang Z, Tawiah B, et al. Recent advances in zinc anodes for high-performance aqueous Zn-ion batteries. *Nano Energy.* 2020;70:104523.
41. Zhang B, Qin L, Fang Y, et al. Tuning  $Zn^{2+}$  coordination tunnel by hierarchical gel electrolyte for dendrite-free zinc anode. *Sci Bull.* 2022;67(9):955-962.
42. Chazalviel J. Electrochemical aspects of the generation of ramified metallic electrodeposits. *Phys Rev A.* 1990;42(12):7355-7367.
43. Barton JL, Bockris JOM. The electrolytic growth of dendrites from ionic solutions. *Proc R Soc London, Ser A Math Phys Sci.* 1962;268(1335):485-505.
44. Ely DR, García RE. Heterogeneous nucleation and growth of lithium electrodeposits on negative electrodes. *J Electrochem Soc.* 2013;160(4):A662-A668.
45. Kim JT, Jorné J. The kinetics and mass transfer of zinc electrode in acidic zinc-chloride solution. *J Electrochem Soc.* 1980;127(1):8-15.
46. Aslam MK, Niu Y, Hussain T, et al. How to avoid dendrite formation in metal batteries: innovative strategies for dendrite suppression. *Nano Energy.* 2021;86:106142.
47. Sand HJSIII. On the concentration at the electrodes in a solution, with special reference to the liberation of hydrogen by electrolysis of a mixture of copper sulphate and sulphuric acid. *Lond Edinb Dubl Phil Mag J Sci.* 2010;1(1):45-79.
48. Li C, Xie X, Liang S, Zhou J. Issues and future perspective on zinc metal anode for rechargeable aqueous zinc-ion batteries. *Energy Environ Mater.* 2020;3(2):146-159.
49. Oniciu L, Mureşan L. Some fundamental aspects of levelling and brightening in metal electrodeposition. *J Appl Electrochem.* 1991;21(7):565-574.
50. Wang X, Mai W, Guan X, et al. Recent advances of electroplating additives enabling lithium metal anodes to applicable battery techniques. *Energy Environ Mater.* 2020;4(3):284-292.
51. Sun X, Zhang X, Ma Q, Guan X, Wang W, Luo J. Revisiting the electroplating process for lithium-metal anodes for lithium-metal batteries. *Angew Chem Int Ed.* 2020;59(17):6665-6674.
52. He P, Huang J. Detrimental effects of surface imperfections and unpolished edges on the cycling stability of a zinc foil anode. *ACS Energy Lett.* 2021;6(5):1990-1995.
53. Zhu R, Xiong Z, Yang H, et al. A low-cost and non-corrosive electropolishing strategy for long-life zinc metal anode in rechargeable aqueous battery. *Energy Storage Mater.* 2022;46:223-232.
54. Zhang Z, Said S, Smith K, et al. Dendrite suppression by anode polishing in zinc-ion batteries. *J Mater Chem A.* 2021;9(27):15355-15362.
55. Yang CP, Yin YX, Zhang SF, Li NW, Guo YG. Accommodating lithium into 3D current collectors with a submicron skeleton towards long-life lithium metal anodes. *Nat Commun.* 2015;6(1):8058.
56. Zeng Y, Zhang X, Qin R, et al. Dendrite-free zinc deposition induced by multifunctional CNT frameworks for stable flexible Zn-ion batteries. *Adv Mater.* 2019;31(36):e1903675.
57. Wang J, Cai Z, Xiao R, et al. A chemically polished zinc metal electrode with a ridge-like structure for cycle-stable aqueous batteries. *ACS Appl Mater Interfaces.* 2020;12(20):23028-23034.
58. Dong L, Yang W, Yang W, et al. Flexible and conductive scaffold-stabilized zinc metal anodes for ultralong-life zinc-ion batteries and zinc-ion hybrid capacitors. *Chem Eng J.* 2020;384:123355.
59. Kang Z, Wu C, Dong L, et al. 3D porous copper skeleton supported zinc anode toward high capacity and long cycle life zinc ion batteries. *ACS Sustain Chem Eng.* 2019;7(3):3364-3371.
60. Wang L-P, Li N-W, Wang T-S, Yin Y-X, Guo Y-G, Wang C-R. Conductive graphite fiber as a stable host for zinc metal anodes. *Electrochim Acta.* 2017;244:172-177.
61. Tian Y, An Y, Wei C, et al. Flexible and free-standing  $Ti_3C_2T_x$  Mxene@Zn paper for dendrite-free aqueous zinc metal batteries and nonaqueous lithium metal batteries. *ACS Nano.* 2019;13(10):11676-11685.
62. Xie X, Liang S, Gao J, et al. Manipulating the ion-transfer kinetics and interface stability for high-performance zinc metal anodes. *Energy Environ Sci.* 2020;13(2):503-510.
63. Shen Z, Luo L, Li C, et al. Stratified zinc-binding strategy toward prolonged cycling and flexibility of aqueous fibrous zinc metal batteries. *Adv Energy Mater.* 2021;11(16):2100214.
64. He H, Qin H, Wu J, et al. Engineering interfacial layers to enable Zn metal anodes for aqueous zinc-ion batteries. *Energy Storage Mater.* 2021;43:317-336.
65. Chu Y, Zhang S, Wu S, Hu Z, Cui G, Luo J. In situ built interphase with high interface energy and fast kinetics for high performance Zn metal anodes. *Energy Environ Sci.* 2021;14(6):3609-3620.

66. Zou P, Zhang R, Yao L, et al. Ultrahigh-rate and long-life zinc-metal anodes enabled by self-accelerated cation migration. *Adv Energy Mater.* 2021;11(31):2100982.
67. Liu Q, Wang Y, Hong X, Zhou R, Hou Z, Zhang B. Elastomer-alginate interface for high-power and high-energy Zn metal anodes. *Adv Energy Mater.* 2022;12(20):2200318.
68. Wu S, Zhang S, Chu Y, Hu Z, Luo J. Stacked lamellar matrix enabling regulated deposition and superior thermo-kinetics for advanced aqueous Zn-ion system under practical conditions. *Adv Funct Mater.* 2021;31(49):2107397.
69. Deng C, Xie X, Han J, et al. A sieve-functional and uniform-porous kaolin layer toward stable zinc metal anode. *Adv Funct Mater.* 2020;30(21):2000599.
70. Hong L, Wu X, Ma C, et al. Boosting the Zn-ion transfer kinetics to stabilize the Zn metal interface for high-performance rechargeable Zn-ion batteries. *J Mater Chem A.* 2021;9(31):16814-16823.
71. Yan H, Li S, Nan Y, Yang S, Li B. Ultrafast zinc-ion-conductor interface toward high-rate and stable zinc metal batteries. *Adv Energy Mater.* 2021;11(18):2100186.
72. Ma L, Li Q, Ying Y, et al. Toward practical high-areal-capacity aqueous zinc-metal batteries: quantifying hydrogen evolution and a solid-ion conductor for stable zinc anodes. *Adv Mater.* 2021;33(12):e2007406.
73. Liu M, Cai J, Ao H, Hou Z, Zhu Y, Qian Y.  $\text{NaTi}_2(\text{PO}_4)_3$  solid-state electrolyte protection layer on Zn metal anode for superior long-life aqueous zinc-ion batteries. *Adv Funct Mater.* 2020;30(50):2004885.
74. Zeng X, Mao J, Hao J, et al. Electrolyte design for in situ construction of highly  $\text{Zn}^{2+}$ -conductive solid electrolyte interphase to enable high-performance aqueous Zn-ion batteries under practical conditions. *Adv Mater.* 2021; 33(11):2007416.
75. Liu H, Wang J-G, Hua W, et al. Navigating fast and uniform zinc deposition via a versatile metal-organic complex interphase. *Energy Environ Sci.* 2022;15(5):1872-1881.
76. Zhao Z, Zhao J, Hu Z, et al. Long-life and deeply rechargeable aqueous Zn anodes enabled by a multifunctional brightener-inspired interphase. *Energy Environ Sci.* 2019;12(6):1938-1949.
77. Zhang Y, Zhu M, Wang G, et al. Dendrites-free Zn metal anodes enabled by an artificial protective layer filled with 2D anionic nanosheets. *Small Methods.* 2021;5(10):e2100650.
78. Hou Z, Gao Y, Tan H, Zhang B. Realizing high-power and high-capacity zinc/sodium metal anodes through interfacial chemistry regulation. *Nat Commun.* 2021;12(1):3083.
79. Li C, Sun Z, Yang T, et al. Directly grown vertical graphene carpets as janus separators toward stabilized Zn metal anodes. *Adv Mater.* 2020;32(33):e2003425.
80. Cao J, Zhang D, Gu C, et al. Modulating Zn deposition via ceramic-cellulose separator with interfacial polarization effect for durable zinc anode. *Nano Energy.* 2021;89:106322.
81. Qin Y, Liu P, Zhang Q, et al. Advanced filter membrane separator for aqueous zinc-ion batteries. *Small.* 2020;16(39): e2003106.
82. Fang Y, Xie X, Zhang B, et al. Regulating zinc deposition behaviors by the conditioner of PAN separator for zinc-ion batteries. *Adv Funct Mater.* 2022;32(14):2109671.
83. Bayaguud A, Luo X, Fu Y, Zhu C. Cationic Surfactant-type electrolyte additive enables three-dimensional dendrite-free zinc anode for stable zinc-ion batteries. *ACS Energy Lett.* 2020; 5(9):3012-3020.
84. Wan F, Zhang L, Dai X, Wang X, Niu Z, Chen J. Aqueous rechargeable zinc/sodium vanadate batteries with enhanced performance from simultaneous insertion of dual carriers. *Nat Commun.* 2018;9(1):1656.
85. Xu W, Zhao K, Huo W, et al. Diethyl ether as self-healing electrolyte additive enabled long-life rechargeable aqueous zinc ion batteries. *Nano Energy.* 2019;62:275-281.
86. Garcia G, Ventosa E, Schuhmann W. Complete prevention of dendrite formation in Zn metal anodes by means of pulsed charging protocols. *ACS Appl Mater Interfaces.* 2017;9(22): 18691-19698.
87. Hou Z, Tan H, Gao Y, Li MH, Lu ZH, Zhang B. Tailoring desolvation kinetics enables stable zinc metal anodes. *J Mater Chem A.* 2020;8(37):19367-19374.
88. Hou Z, Gao Y, Zhou R, Zhang B. Unraveling the rate-dependent stability of metal anodes and its implication in designing cycling protocol. *Adv Funct Mater.* 2021;32(7): 2107584.
89. Cao L, Li D, Hu E, et al. Solvation structure design for aqueous Zn metal batteries. *J Am Chem Soc.* 2020;142(51):21404-21409.
90. Blanc LE, Kundu D, Nazar LF. Scientific challenges for the implementation of Zn-ion batteries. *Joule.* 2020;4(4):771-799.
91. Singh V, Singh D. An overview on the preparation, characterization and properties of electrodeposited-metal matrix nanocomposites. *Nanosci Technol.* 2014;1(3):1-20.
92. Xie F, Li H, Wang X, et al. Mechanism for zincophilic sites on zinc-metal anode hosts in aqueous batteries. *Adv Energy Mater.* 2021;11(9):2003419.
93. Foroozan T, Yurkiv V, Sharifi-Asl S, Rojaee R, Mashayek F, Shahbazian-Yassar R. Non-dendritic Zn electrodeposition enabled by zincophilic graphene substrates. *ACS Appl Mater Interfaces.* 2019;11(47):44077-44089.
94. Zheng J, Zhao Q, Tang T, et al. Reversible epitaxial electrodeposition of metals in battery anodes. *Science.* 2019;366(6465): 645-648.
95. Cui M, Xiao Y, Kang L, et al. Quasi-isolated Au particles as heterogeneous seeds to guide uniform Zn deposition for aqueous zinc-ion batteries. *ACS Appl Energy Mater.* 2019;2(9): 6490-6496.
96. Han D, Wu S, Zhang S, et al. A corrosion-resistant and dendrite-free zinc metal anode in aqueous systems. *Small.* 2020;16(29):e2001736.
97. Guo W, Cong Z, Guo Z, et al. Dendrite-free Zn anode with dual channel 3D porous frameworks for rechargeable Zn batteries. *Energy Storage Mater.* 2020;30:104-112.
98. Shi X, Xu G, Liang S, et al. Homogeneous deposition of zinc on three-dimensional porous copper foam as a superior zinc metal anode. *ACS Sustain Chem Eng.* 2019;7(21):17737-17746.
99. Zhao J, Ren H, Liang Q, et al. High-performance flexible quasi-solid-state zinc-ion batteries with layer-expanded vanadium oxide cathode and zinc/stainless steel mesh composite anode. *Nano Energy.* 2019;62:94-102.
100. Cui Y, Zhao Q, Wu X, et al. An interface-bridged organic-inorganic layer that suppresses dendrite formation and side reactions for ultra-long-life aqueous zinc metal anodes. *Angew Chem Int Ed.* 2020;59(38):16594-16601.

101. Yang H, Chang Z, Qiao Y, et al. Constructing a super-saturated electrolyte front surface for stable rechargeable aqueous zinc batteries. *Angew Chem Int Ed.* 2020;59(24):9377-9381.
102. Yuksel R, Buyukcakir O, Seong WK, Ruoff RS. Metal-organic framework integrated anodes for aqueous zinc-ion batteries. *Adv Energy Mater.* 2020;10(16):1904215.
103. Yang Q, Guo Y, Yan B, et al. Hydrogen-substituted graphdiyne ion tunnels directing concentration redistribution for commercial-grade dendrite-free zinc anodes. *Adv Mater.* 2020;32(25):e2001755.
104. Cao J, Zhang D, Gu C, et al. Manipulating crystallographic orientation of zinc deposition for dendrite-free zinc ion batteries. *Adv Energy Mater.* 2021;11(29):2101299.
105. Zhang Y, Howe JD, Ben-Yoseph S, Wu Y, Liu N. Unveiling the origin of alloy-seeded and nondendritic growth of Zn for rechargeable aqueous Zn batteries. *ACS Energy Lett.* 2021;6(2):404-412.
106. Wang F, Borodin O, Gao T, et al. Highly reversible zinc metal anode for aqueous batteries. *Nat Mater.* 2018;17(6):543-549.
107. Zhang C, Holoubek J, Wu X, et al. A ZnCl<sub>2</sub> water-in-salt electrolyte for a reversible Zn metal anode. *Chem Commun.* 2018;54(100):14097-14099.
108. Zhu Y, Yin J, Zheng X, et al. Concentrated dual-cation electrolyte strategy for aqueous zinc-ion batteries. *Energy Environ Sci.* 2021;14(8):4463-4473.
109. Chen CY, Matsumoto K, Kubota K, Hagiwara R, Xu Q. A room-temperature molten hydrate electrolyte for rechargeable zinc-air batteries. *Adv Energy Mater.* 2019;9(22):1900196.
110. Chen S, Lan R, Humphreys J, Tao S. Salt-concentrated acetate electrolytes for a high voltage aqueous Zn/MnO<sub>2</sub> battery. *Energy Storage Mater.* 2020;28:205-215.
111. Li W, Wang K, Zhou M, Zhan H, Cheng S, Jiang K. Advanced low-cost, high-voltage, long-life aqueous hybrid sodium/zinc batteries enabled by a dendrite-free zinc anode and concentrated electrolyte. *ACS Appl Mater Interfaces.* 2018;10(26):22059-22066.
112. Chen S, Nian Q, Zheng L, et al. Highly reversible aqueous zinc metal batteries enabled by fluorinated interphases in localized high concentration electrolytes. *J Mater Chem A.* 2021;9(39):22347-22352.
113. Hao J, Yuan L, Ye C, et al. Boosting zinc electrode reversibility in aqueous electrolytes by using low-cost antisolvents. *Angew Chem Int Ed.* 2021;60(13):7366-7375.
114. Chang N, Li T, Li R, et al. An aqueous hybrid electrolyte for low-temperature zinc-based energy storage devices. *Energy Environ Sci.* 2020;13(10):3527-3535.
115. Zhang Y, Zhu M, Wu K, et al. An in-depth insight of a highly reversible and dendrite-free Zn metal anode in an hybrid electrolyte. *J Mater Chem A.* 2021;9(7):4253-4261.
116. Naveed A, Yang H, Yang J, Nuli Y, Wang J. Highly Reversible and rechargeable safe Zn batteries based on a triethyl phosphate electrolyte. *Angew Chem Int Ed.* 2019;58(9):2760-2764.
117. Naveed A, Yang H, Shao Y, et al. A highly reversible Zn anode with intrinsically safe organic electrolyte for long-cycle-life batteries. *Adv Mater.* 2019;31(36):e1900668. doi:10.1002/adma.201900668
118. Qiu X, Wang N, Dong X, et al. A high-voltage Zn-organic battery using a nonflammable organic electrolyte. *Angew Chem Int Ed.* 2021;60(38):21025-21032.
119. Hao J, Long J, Li B, et al. Toward high-performance hybrid Zn-based batteries via deeply understanding their mechanism and using electrolyte additive. *Adv Funct Mater.* 2019;29(34):1903605.
120. Jin Y, Han KS, Shao Y, et al. Stabilizing zinc anode reactions by polyethylene oxide polymer in mild aqueous electrolytes. *Adv Funct Mater.* 2020;30(43):2003932.
121. Zhang Q, Luan J, Fu L, et al. The three-dimensional dendrite-free zinc anode on a copper mesh with a zinc-oriented polyacrylamide electrolyte additive. *Angew Chem Int Ed.* 2019;58(44):15841-15847.
122. Qiu H, du X, Zhao J, et al. Zinc anode-compatible in-situ solid electrolyte interphase via cation solvation modulation. *Nat Commun.* 2019;10(1):5374. doi:10.1038/s41467-019-13436-3
123. Dong Y, Miao L, Ma G, et al. Non-concentrated aqueous electrolytes with organic solvent additives for stable zinc batteries. *Chem Sci.* 2021;12(16):5843-5852. doi:10.1039/d0sc06734b
124. Wang L, Zhang Y, Hu H, et al. A Zn(ClO<sub>4</sub>)<sub>2</sub> electrolyte enabling long-life zinc metal electrodes for rechargeable aqueous zinc batteries. *ACS Appl Mater Interfaces.* 2019;11(45):42000-42005.
125. Hao J, Li X, Zhang S, et al. Designing dendrite-free zinc anodes for advanced aqueous zinc batteries. *Adv Funct Mater.* 2020;30(30):2001263.
126. Zhou M, Guo S, Fang G, et al. Suppressing by-product via stratified adsorption effect to assist highly reversible zinc anode in aqueous electrolyte. *J Energy Chem.* 2021;55:549-556.
127. Zhao R, Yang Y, Liu G, et al. Redirected Zn electrodeposition by an anti-corrosion elastic constraint for highly reversible Zn anodes. *Adv Funct Mater.* 2020;31(2):2001867.
128. Cai Z, Ou Y, Wang J, et al. Chemically resistant Cu-Zn/Zn composite anode for long cycling aqueous batteries. *Energy Storage Mater.* 2020;27:205-211.
129. Sun KE, Hoang TK, Doan TN, et al. Suppression of dendrite formation and corrosion on zinc anode of secondary aqueous batteries. *ACS Appl Mater Interfaces.* 2017;9(11):9681-9687. doi:10.1021/acsami.6b16560
130. Leng K, Li G, Guo J, et al. A safe polyelectrolyte hydrogel electrolyte for long-life quasi-solid state zinc metal batteries. *Adv Funct Mater.* 2020;30(23):2001317.
131. Hou Z, Lu Z, Chen Q, Zhang B. Realizing wide-temperature Zn metal anodes through concurrent interface stability regulation and solvation structure modulation. *Energy Storage Mater.* 2021;42:517-525.
132. Zhang XQ, Cheng XB, Chen X, Yan C, Zhang Q. Fluoroethylene carbonate additives to render uniform Li deposits in lithium metal batteries. *Adv Funct Mater.* 2017;27(10):1605989.
133. Liu Z, Yang Y, Liang S, Lu B, Zhou J. pH-buffer contained electrolyte for self-adjusted cathode-free Zn-MnO<sub>2</sub> batteries with coexistence of dual mechanisms. *Small Struct.* 2021;2(11):2100119.
134. Sasaki Y, Yoshida K, Kawasaki T, Kuwabara A, Ukyo Y, Ikuhara Y. In situ electron microscopy analysis of electrochemical Zn deposition onto an electrode. *J Power Sources.* 2021;481:228831.
135. Grey CP, Tarascon JM. Sustainability and in situ monitoring in battery development. *Nat Mater.* 2016;16(1):45-56.
136. Deng Z, Huang Z, Shen Y, et al. Ultrasonic scanning to observe wetting and "unwetting" in Li-ion pouch cells. *Joule.* 2020;4(9):2017-2029.

137. Zhang J, Lee J. A review on prognostics and health monitoring of Li-ion battery. *J Power Sources*. 2011;196(15):6007-6014.
138. Huang J, Han X, Liu F, et al. Monitoring battery electrolyte chemistry via in-operando tilted fiber Bragg grating sensors. *Energy Environ Sci*. 2021;14(12):6464-6475.
139. Huang J, Albero Blanquer L, Bonefacino J, et al. Operando decoding of chemical and thermal events in commercial Na (Li)-ion cells via optical sensors. *Nat Energy*. 2020;5(9):674-683.
140. Yang Q, Liang G, Guo Y, et al. Do zinc dendrites exist in neutral zinc batteries: a developed electrohealing strategy to in situ rescue in-service batteries. *Adv Mater*. 2019;31(43):e1903778.

## AUTHOR BIOGRAPHIES



**Zhen Hou** is currently a PhD student in The Hong Kong Polytechnic University. He received BE and MS degrees from Harbin Institute of Technology in 2017 and 2019, respectively. His research interests focus on

alkali and alkaline earth metal anodes, especially the electrochemical interfaces between anode and electrolyte.



**Biao Zhang** received his PhD from the Hong Kong University of Science and Technology. He was a postdoc fellow in College de France before joining the Hong Kong Polytechnic University in 2017. His recent work focus on building and probing robust electrode/electrolyte interfaces for rechargeable metal-ion batteries.

**How to cite this article:** Hou Z, Zhang B. Boosting Zn metal anode stability: from fundamental science to design principles. *EcoMat*. 2022;4(6):e12265. doi:[10.1002/eom2.12265](https://doi.org/10.1002/eom2.12265)